THE JOURNAL OF PHYSICAL CHEMISTRY A

 VOLUME 112, NUMBER 41, OCTOBER 16, 2008

CENTENNIAL FEATURE ARTICLE

Statistical Rate Theory and Kinetic Energy-Resolved Ion Chemistry: Theory and Applications†

P. B. Armentrout,* Kent M. Ervin, and M. T. Rodgers

Received: June 17, 2008

Ion chemistry, first discovered 100 years ago, has profitably been coupled with statistical rate theories, developed about 80 years ago and refined since. In this overview, the application of statistical rate theory to the analysis of kinetic-energy-dependent collision-induced dissociation (CID) reactions is reviewed. This procedure accounts for and quantifies the kinetic shifts that are observed as systems increase in size. The statistical approach developed allows straightforward extension to systems undergoing competitive or sequential dissociations. Such methods can also be applied to the reverse of the CID process, association reactions, as well as to quantitative analysis of ligand exchange processes. Examples of each of these types of reactions are provided and the literature surveyed for successful applications of this statistical approach to provide quantitative thermochemical information. Such applications include metal−ligand complexes, metal clusters, proton-bound complexes, organic intermediates, biological systems, saturated organometallic complexes, and hydrated and solvated species.

Introduction

Shortly after the physical division of the American Chemical Society was established, J. J. Thompson observed the first ion−molecule reaction, $H_2^+ + H_2 \rightarrow H_3^+ + H$.[1] Statistical expressions for the rates of chemical reactions are nearly as old, having been developed by Rice and Ramsperger[2,3] and Kassel[4] (RRK) about 80 years ago. These approaches laid the groundwork for more advanced schemes still in use today, as developed independently by Marcus[5,6] (RRKM) and Eyring and co-workers[7] just over half a century ago. Indeed, Eyring's approach, quasi equilibrium theory (QET), was developed specifically to explain the behavior of ionized polyatomic molecules. Thus, ever since the inception of statistical theories in chemistry, the scientific community interested in ion−molecule reactions has embraced and exploited them.

Eyring's initial application of statistical rate theory to ionic systems[7] involved predicting the fragmentation patterns of ions produced by electron impact ionization in mass spectrometers, typically at excess electron energies of 50−70 eV. Later, statistical effects were found to be particularly important in appearance energy measurements, where the onset of parent ions and fragment ions is measured as a function of electron energy (or photon energy in photoionization experiments), because of the lower energy and therefore longer dissociation lifetimes relative to detection time windows. For dissociative photoionization threshold measurements, Chupka[8] described the "kinetic shifts" that could result from delayed unimolecular dissociation following ionization. Lifshitz and Long[9] discussed the threshold shifts resulting from competition among several fragmentation product channels, i.e., "competitive shifts", for appearance energy measurements using electron ionization. Unfortunately, early appearance energy measurements using electron ionization often suffered from large inaccuracies, poor experimental control over energy distributions and detection efficiencies, and practical difficulties in modeling the kinetic and competitive shifts.[10] In recent decades, increasingly sophisticated statistical rate theories have been used to model ion−molecule reactions, photoionization, and photodissociation of ions.[11]

† This year marks the Centennial of the American Chemical Society's Division of Physical Chemistry. To celebrate and to highlight the field of physical chemistry from both historical and future perspectives, *The Journal of Physical Chemistry* is publishing a special series of Centennial Feature Articles. These articles are invited contributions from current and former officers and members of the Physical Chemistry Division Executive Committee and from *J. Phys. Chem.* Senior Editors.

10.1021/jp805343h CCC: $40.75
Published on Web 09/23/2008

Peter B. Armentrout is a Distinguished Professor of Chemistry and Cannon Fellow in the Department of Chemistry at the University of Utah. After receiving a B.S. degree from Case Western Reserve University in 1975, he obtained his Ph.D. in chemistry from Caltech in 1981, working with Prof. J. L. Beauchamp. After a postdoc at Bell Laboratories, he joined the faculty at the University of California, Berkeley and then the University of Utah. Dr. Armentrout's research group uses guided ion beam tandem mass spectrometry and computational approaches to study the thermodynamics, kinetics, dynamics, and spectroscopy of reaction systems ranging from organometallic chemistry, transition metal clusters, hydration, and biological systems.

Kent M. Ervin obtained his Ph.D. degree in Physical Chemistry from the University of California, Berkeley, in 1986, working with Prof. P. B. Armentrout. After a post-doctoral research position with Prof. W. C. Lineberger at JILA in Boulder, CO, he joined the faculty of the University of Nevada, Reno, where he is currently a Professor in the Department of Chemistry and the Chemical Physics Program. Dr. Ervin's research interests include ion−molecule reaction kinetics and dynamics and ion spectroscopy.

Mary T. Rodgers obtained B.S. degrees in Chemistry and Mathematics in 1985 from Illinois State University. She earned her Ph.D. in Chemical Physics from the California Institute of Technology, Pasadena, in 1992, working with Prof. A. Kuppermann. She remained at Caltech to pursue postdoctoral work with Prof. J. L. Beauchamp until 1994, when she moved on to the University of Utah, Salt Lake City, also as a postdoctoral fellow, to work with Prof. P. B. Armentrout. She joined the faculty at Wayne State University, Detroit, MI, in 1997, where she is currently a Professor of Physical and Analytical Chemistry, and the Analytical Division Head. Dr. Rodgers' research interests involve the application of physical and analytical mass spectrometry techniques complemented by theory to study ion−molecule reactions, collision-induced dissociation, and infrared multiphoton dissociation to examine the structures, dynamics, kinetics, and thermochemistry of biological and organic molecules, metal−ligand complexes, and solvation.

Of particular note, Bowers, Chesnavich, and co-workers[12−19] pioneered the development of statistical rate theory methods for metastable ion dissociation and for translationally driven ion−molecule reactions.

Lifshitz has pointed out that because ions can be produced with well-defined internal energies at low pressures in the absence of molecular collisions, there are intrinsic advantages of using ions to address fundamental problems associated with rate theory.[20] In our laboratories, we have exploited yet another feature of ions that provides additional advantages coupled with new challenges. Specifically, the kinetic energy of ions can be varied over a very wide range (at least 4 orders of magnitude), thereby allowing ion chemistry to be examined at much higher collision energies than can be accessed using thermal techniques. This large range of energies is available because of the advent of radio frequency (rf) ion guide technology;[21,22] otherwise ion chemistry cannot be studied easily at energies below about 1 eV in the laboratory frame. In our laboratories, the use of octopole ion beam guides provides the ability to access such low energies while retaining good ion intensity and facile measurement of the absolute energy and energy distribution of the ion beam.[23] Although this review illustrates applications of statistical rate theory to gas-phase ion−molecule reactions studied as a function of kinetic energy by focusing primarily on work in our laboratories, many others have also made contributions to statistical rate modeling of ion−molecule reactions and we include some of those examples as well. Because of space limitations, we exclude photoionization, electron ionization or capture, and multiple-collision activation processes, but statistical rate modeling has also been important for those techniques.

Fundamental Assumptions of Statistical Rate Theories. The key assumptions of statistical rate theories[11,24] include (1) there exists a hypersurface in phase space that divides reactants and products in a way that minimizes the probability that products can recross this surface to reform reactants (indeed, this probability is assumed to be zero); (2) all microstates of the system have an equal probability of being populated such that the rate depends only on the total energy and total angular momentum (the ergodic assumption in which there are no dynamical effects). Assumption 2 implies that intramolecular vibrational relaxation (IVR) is rapid compared with the reaction rate. Leitner, Wolynes, and co-workers[25,26] have shown that is not always the case, for example, in the rapid isomerization of moderately large systems with low energy barriers. Microcanonical statistical rate theory also implicitly assumes that no energy is exchanged between the reactants and the environment during the dissociation process, i.e., low-pressure conditions with no radiative absorption or emission. Those conditions usually apply to the collision-induced processes considered here, which are measured in the single-collision limit and occur on time scales of about 10^{-4} s or faster. In contrast, the blackbody infrared dissociation (BIRD) technique[27,28] takes advantage of radiative activation of ions stored for much longer time periods. In the approaches detailed below for describing collision-induced ion−molecule chemistry, the statistical assumption is applied repeatedly, which ultimately is the least biased assumption that can be made. Clearly, in systems that involve dynamical constraints and effects, deviations from statistical behavior can be observed, but formulating a *general* theory for such systems is impossible.

Statistical Approach to Collision-Induced Dissociation. The utilization of statistical approaches in understanding collision-induced dissociation (CID) starts with breaking the CID process, reaction 1,

$$ABC^+ + M \rightarrow AB^+ + C + M \quad (1)$$

into two steps: collisional excitation of the ABC^+ reactant with another species M to form the $ABC^{+}*$ energized molecule (EM), reaction 2a, which then undergoes unimolecular decomposition through the $ABC^{+\dagger}$ transition state (TS), reaction 2b.

$$ABC^+ + M \rightarrow ABC^{+}* + M \quad (2a)$$

$$ABC^{+}* \rightarrow ABC^{+\dagger} \rightarrow AB^+ + C \quad (2b)$$

Clearly the second step (eq 2b) can be treated using the standard statistical assumptions associated with transition-state theory in all its variants, such as RRKM theory, presuming that the internal energy (E^*) and rotational angular momentum (J^*) of $ABC^{+}*$ are known. The assumptions associated with the collisional first step are crucial and can be treated using simple collision theory and statistical assumptions. These assumptions are outlined in the next section, which focuses on the energy deposition function, i.e., the probability that a single collision will deposit a specific amount of energy into the ABC^+ molecule.

Energy Deposition Function. To a first approximation, the kinetic energy dependence of collisional processes can be considered in terms of the line-of-centers model, eq 3, which includes conservation of both linear and angular momenta for the case of hard spheres. Here, the energy barrier along the potential energy surface is represented by E_0, E is the relative kinetic energy of the reactants, and σ_0 is a scaling factor that is generally thought of as the collision cross section ($\sigma_0 = \sigma d^2$ for hard spheres, where d is the sum of the hard-sphere radii of the reactants).

$$\sigma(E) = \sigma_0(E - E_0)/E \quad (3)$$

Using microscopic reversibility and the Langevin−Gioumousis−Stevenson (LGS) collision model for ion−molecule reactions,[29] one can derive[30] eq 4 for the case of reactions endothermic by or having a barrier of E_0, where $\sigma_0 = \pi e(\alpha/2\pi\varepsilon_0)^{1/2}$, α is the polarizability of the neutral reactant in volume units (the SI polarizability divided by $4\pi\varepsilon_0$), e is the

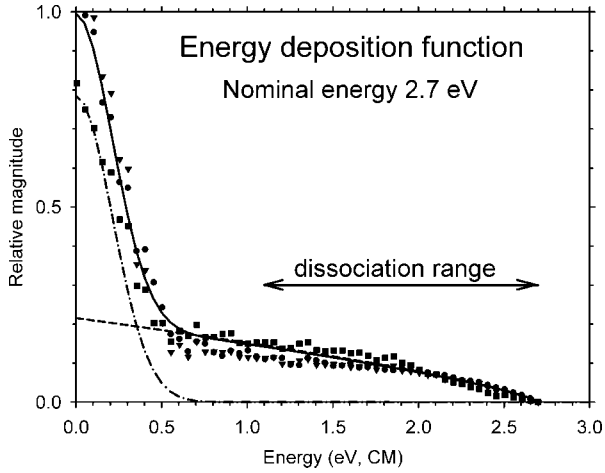

Figure 1. Deposited energy distribution measured for $Cr(CO)_6^+$ ions as a result of collisions with Xe at a pressure of 0.1 mTorr at a collision energy of 2.7 eV, obtained from experimental velocity maps. The different sets of points are the result of the different procedures performed to the Cartesian velocity maps before converting into CM energy distributions. The energy region over which dissociation is possible is represented by the arrows. The dashed line represents the best fit to the data using the equation $P(\varepsilon) = \sigma_0 n(E - \varepsilon)^{n-1}/E$ with $n = 1.75$. The low-energy peak of the distribution corresponds to the contribution of unscattered primary ions and is reproduced with a Gaussian (dash-dot line). Data taken from ref 32.

charge of an electron, and ε_0 is the permittivity of vacuum.

$$\sigma(E) = \sigma_0(E - E_0)^{1/2}/E \tag{4}$$

Furthermore, Bowers and co-workers[14] have derived an expression for the cross section of "translationally driven reactions" and obtained eq 5,

$$\sigma(E) = \sigma_0(E - E_0)^{(\Delta v+2)/2}/E \tag{5}$$

where Δv is the number of vibrational degrees of freedom created upon formation of the TS from reactants. For hard spheres, $\Delta v = 0$ and one recovers eq 3, as one should. A variety of other expressions for the energy dependence of reaction cross sections have been derived, as discussed thoroughly elsewhere,[31] but in most cases they can be parametrized in terms of eq 6, the so-called modified line-of-centers expression where n is a variable parameter.

$$\sigma(E) = \sigma_0(E - E)^n/E \tag{6}$$

This expression is assumed to accurately represent the kinetic energy dependence of the initial collisional activation process at hyperthermal energies.

As shown elsewhere,[32] the cross section expression in eq 6 can be written equivalently in terms of an energy deposition function, $P_E(\varepsilon) = \sigma_0 n(E - \varepsilon)^{n-1}/E$, where ε is the energy deposited into internal modes of the EM during the excitation collision. This yields eq 7.

$$\sigma(E) = \int_{E_0}^{E} P_E(\varepsilon)\, d\varepsilon = (\sigma_0 n/E)\int_{E_0}^{E} (E - \varepsilon)^{n-1}\, d\varepsilon \tag{7}$$

Note that the energy deposition function $P_E(\varepsilon)$ is a constant (σ_0/E) when $n = 1$ (as appropriate for hard spheres; i.e., $\sigma(E)$ is given by eq 3), properly reflecting that the probability of a collision at a specific energy is a constant function of the impact parameter for hard spheres. Importantly, the utility of this expression has been directly demonstrated by experimentally measuring the energy deposition function for the case of $Cr(CO)_6^+$ colliding with Xe.[32] The results of this study are reproduced in Figure 1. Note that these data demonstrate the critical result that there is a finite probability of depositing *all* of the relative kinetic energy into internal energy of the EM, which is a requirement for threshold energies to be meaningful thermodynamic quantities. In addition, this model of the energy dependence of reaction cross sections has accurately determined the shapes of a multitude of experimental cross sections.[33−35] Although the model requires the use of an empirical parameter n, experiments over the past decades establish that no single value of this parameter is appropriate for all systems and that even simple predictions, such as $n = (\Delta v + 2)/2$ (eq 5), are not accurate.

In real experiments, the reactant ABC^+ molecule begins with a distribution of internal energies (as could the collision partner M), which is assumed to be available for further reaction, process 2b, and therefore needs to be included. This is accomplished by introducing a summation over the rovibrational states i of the reactants with populations g_i, where $\Sigma g_i = 1$, yielding eq 8.

$$\sigma(E) = \sigma_0 \sum_i g_i (E + E_i - E_0)^n/E$$
$$= (\sigma_0 n/E)\sum_i g_i \int_{E_0 - E_i}^{E} (E - \varepsilon)^{n-1}\, d\varepsilon \tag{8}$$

This gives $E + E_i$ as the total energy available to the colliding reactants and means that reaction 2b can occur if $E^* = \varepsilon + E_i \geq E_0$; i.e., $\varepsilon \geq E_0 - E_i$ is transferred in the collision. Vibrational frequencies and rotational constants used to calculate E_i and g_i are obtained from literature experiments or calculations. The Beyer−Swinehart−Stein−Rabinovitch algorithm[36−38] is used to evaluate the density of the rovibrational states and the relative populations g_i are calculated for the distribution appropriate for the particular experimental conditions. In most of our experiments, this is a Boltzmann distribution at 300 K.

Unimolecular Dissociation. Given this model for the collisional cross section associated with reaction 2a, the probability of the unimolecular dissociation reaction 2b, $P_D(\varepsilon)$, now needs to be introduced. This dissociation probability is given by $[1 - e^{-k(E^*)\tau}]$, where $k(E^*)$ is the unimolecular rate constant for dissociation, τ is the experimental time for dissociation (approximately 10^{-4} s in the instrumentation used in our laboratories) and, as noted above, E^* is the internal energy of the energized molecule (EM) after the collision. This transforms eq 8 into eq 9.

$$\sigma(E) = \int P_E(\varepsilon)\, P_D(\varepsilon)\, d\varepsilon$$
$$= (\sigma_0 n/E)\sum_i g_i \int_{E_0 - E_i}^{E} [1 - e^{-k(\varepsilon + E_i)\tau}] \times (E - \varepsilon)^{n-1}\, d\varepsilon \tag{9}$$

Note that $P_D(\epsilon)$ falls inside the integral as the dissociation probability depends critically on ε. The term $k(E^*) = k(\varepsilon + E_i)$ is assigned to the unimolecular rate constant for dissociation as defined by Rice−Ramsperger−Kassel−Marcus (RRKM) theory, eq 10,

$$k(E^*,J) = dN_{vr}^{\dagger}(E^* - E_0,J)/h\rho_{vr}(E^*,J) \tag{10}$$

where d is the reaction degeneracy, $N_{vr}^{\dagger}(E^* - E_0,J)$ is the sum of rovibrational states of the TS, $\rho_{vr}(E^*,J)$ is the density of rovibrational states of the EM, J is the total angular momentum of the postcollision EM, and h is Planck's constant.[11,39,40] Variants of RRKM theory treat angular momentum effects in different ways.[11] In phase space theory (PST),[41−43] the sum and density of states are calculated with explicit conservation of angular momentum as well as energy. Rodgers, Ervin, and Armentrout[44] discussed several possible treatments of the 2D external rotations of the EM, but for CID processes, it is often sufficient to use an approximation in which the 2D external

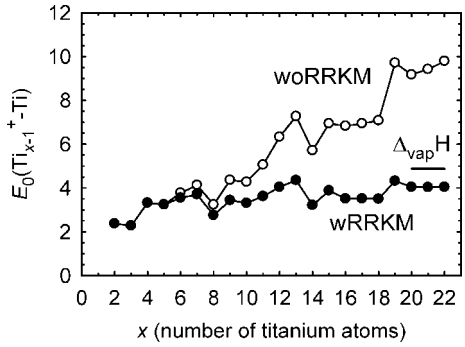

Figure 2. Collision-induced dissociation thresholds of titanium cluster cations determined including (solid symbols) and excluding (open symbols) RRKM estimates of kinetic shifts. The horizontal bar indicates the bulk-phase vaporization enthalpy of titanium. Data taken from ref 47.

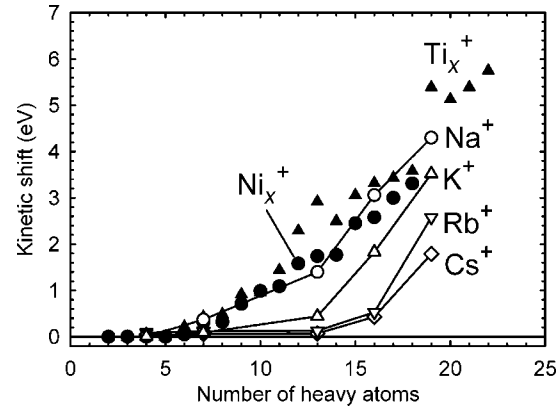

Figure 3. Kinetic shifts determined in threshold CID experiments as a function of the number of heavy atoms in transition metal cluster systems (Ti_x^+ and Ni_x^+, solid symbols) and alkali cation ether complexes (open symbols).

rotations of the complex are treated as adiabatic and the energy of that rotation is excluded from promoting reaction. This treatment, which follows that outlined by Waage and Rabinovitch,[45] yields eq 11.

$$k(E^*,J) = dN_{vr}^{\dagger}(E^* - E_R^{\dagger}(J) - E_0)/h\rho_{vr}(E^* - E_R(J)) \quad (11)$$

The rotational energies $E_R^{\dagger}(J)$ and $E_R(J)$ are the 2D external rotational energies of the TS and EM, respectively. The rotational energies at the TS, $E_R^{\dagger}(J)$, differ from those for the EM, $E_R(J)$, because the 2D rotational constant B decreases as the molecule dissociates. (This is easily seen by noting that $B \propto 1/I \sim 1/\mu r^2$, where I is the moment of inertia, μ is the reduced mass of the separating products, and r is their separation.) The distribution of J in the postcollision EM is discussed more thoroughly in the next section. In the limit that $k(E^*,J)$ is much faster than the experimental time available for dissociation of the ions, the term in square brackets in eq 9 reduces to unity, recovering eq 8.

The need for including the unimolecular dissociation lifetime of the EM in CID threshold analyses became obvious in analyzing the dissociation behavior of transition metal clusters.[46] Figure 2 shows threshold energies obtained from analysis of data for titanium cluster cations[47] with and without including RRKM theory. It can be seen that without the treatment of kinetic shifts included, the threshold energies, which should be equivalent to the bond dissociation energies (BDEs) for removing a single titanium atom from the cluster of size x, begin to exceed the bulk-phase asymptotic value of $\Delta_{vap}H_0$(Ti). Once kinetic shifts are properly included in the model, the threshold values converge to the bulk-phase value (a convergence that is more easily demonstrated using a spherical drop model that plots the average atomization energies as a function of $x^{1/3}$).[47] This conclusion is true for all metal clusters studied by the Armentrout group.[48]

The magnitudes of the kinetic shifts depend on three primary quantities: the experimental time scale (τ), the number of degrees of freedom in the EM, and the threshold energy. Figure 3 shows how the kinetic shift increases with the former quantity for two types of systems: metal cluster cations, Ti_x^+ and Ni_x^+,[47,49] and alkali metal cationized crown ethers, $M^+(c\text{-}C_2H_4O)_y$ ($y = 4$–6), and related complexes, $M^+(CH_2OCH_3)_2$ and $M^+(CH_3OCH_3)$.[50] In both cases, the effective degrees of freedom are roughly related to the number of heavy atoms in the system (excluding hydrogen), which deemphasizes the high-frequency vibrations of hydrogen atoms that contribute less to the density and number of states than low-frequency motions. The correspondence between the kinetic shifts found for the metal cluster cations and Na^+ complexes shows that the dependence on degrees of freedom is largely independent of the kind of system considered. The variations with alkali metal cation identity illustrate how the kinetic shifts vary with threshold energy, i.e., the bond energies of the $M^+(c\text{-}C_2H_4O)_y$ complexes become systematically weaker as the size of the metal cation increases. For example, for $y = 6$ (18-crown-6), the metal ligand bond energies are 3.07 ± 0.20 eV for $M^+ = Na^+$, 2.43 ± 0.13 eV for K^+, 1.98 ± 0.13 eV for Rb^+, and 1.74 ± 0.09 eV for Cs^+. Thus, the kinetic shifts become smaller as the same number of heavy atoms is retained.

The magnitude and energy dependence of statistical rate constants are very sensitive to the TS energies, but much less sensitive to vibrational and rotational frequency parameters. Errors in the vibrational frequencies often cancel in the ratio of the sum and density of states in eq 11. Therefore, theoretical methods used to calculate frequencies do not need to be particularly sophisticated to accurately model the statistical rates. That makes the statistical rate models especially advantageous for experimental determinations of energetics, which can be challenging even for sophisticated theoretical methods.

Distribution of External Rotations. As noted above, experiments have demonstrated that eq 7 can be used to determine the approximate distribution of energies in the EM, i.e., E^*. To accurately calculate $k(E^*,J)$ in eq 11, the distribution of J is also required. For bimolecularly formed intermediate complexes or association reactions, J is often equated to the collision orbital angular momentum L, and its distribution is then fixed exactly by the random distribution of impact parameters, i.e., $P(J) = 1/J_{max}$, where J_{max}, defined as $J_{max}(J_{max} + 1) = (2\mu^2\alpha e^2 E/\pi\varepsilon_0\hbar^4)^{1/2}$, is related to the maximum impact parameter for which reactants can overcome the centrifugal barrier on the ion−induced-dipole long-range potential. For collision-induced dissociation, the departing target gas atom can carry off some of the initial orbital angular momentum and no direct information is available to assess the distribution of J values after the activating collision. Rodgers, Ervin, and Armentrout[44] discussed various options and recommended a statistical approximation that assumes all vibrational and rotational states at the total energy of the EM are equally accessible. A statistical distribution is appropriate in the limit that the orbital angular momentum in the initial collision between the reactant ion and the collision target is conserved during the excitation collision; i.e., there is no strong coupling between the external 2D rotation of the transient complex formed between the ion complex and collision target and its internal degrees of freedom. In this statistical approximation,[44,61] the entire dissociation probability is averaged over the quantum number J for the inactive 2D external rotations, weighted by the density of states of the remaining rovibrational states, eq 12,

$$P_D(\varepsilon) = \langle 1 - e^{-k(E^*,J)\tau} \rangle = \sum_{J=0}^{J_{max}} [1 - e^{-k(E^*,J)\tau}] \times g_J \rho_{vr}(E^* - E_R(J)) / \sum_{J=0}^{J_{max}} g_J \rho_{vr}(E^* - E_R(J)) \quad (12)$$

where most of the terms are defined above and $g_J = (2J + 1)$ is the degeneracy of the 2D rotor. $J_{max} = ((1 + 4E^*/hcB)^{1/2} - 1)/2$, the maximum value possible for the rotational quantum number determined by energy conservation, is derived from the definition of the rotational energy, $E_R(J) = hcBJ(J + 1)$. The expression for $P_D(\varepsilon)$ in eq 12 is substituted for the term in square brackets in eq 9. Ultimately, experimental CID results have not been found to be particularly sensitive to the choice made for the treatment of rotations. Because it is the least biased approach, using the statistical distribution of eq 12 is our recommended method (with either eq 11 or PST for treatment of rotations in the statistical rate calculations). However, association reactions, described more fully below, verify that this choice is also likely to be the most accurate treatment of rotations.

Transition States. The nature of the transition state (TS) can strongly influence the rate constants calculated by statistical rate theory. One limiting case is a "tight", fixed vibrator TS, which is modeled as a collection of oscillators. Here, frequencies can be estimated as similar to the dissociating molecule, except one is removed as the reaction coordinate and usually four others reduced as transitional modes. Alternatively, explicit theoretical calculations can be used to identify the vibrational frequencies of the tight TS. The other limiting case is a "loose", orbiting TS (aka phase space limit or PSL TS), which models the system with the frequencies of the free products.[39] Here, five degrees of freedom are usually treated as rotations of the independent product molecules.

When the TS is tight, $B^\dagger$ (the 2D rotational constant of the TS) is well-defined and therefore $E_R^\dagger(J)$ is easily evaluated. A test of the statistical analysis for such a system is the decarbonylation of phenol cation, $C_6H_5OH^+ \rightarrow C_5H_6^+ + CO$, which is known to involve a tight TS associated with an initial enol-keto isomerization. Literature values for the activation energy required for this process are 3.12 ± 0.10 eV from photoelectron photoion coincidence (PEPICO) studies,[51] 2.98 ± 0.10 eV from reanalysis of the PEPICO data,[52] 3.16 ± 0.10 eV from time-resolved electron impact measurements,[53] 2.93 ± 0.04 eV from photoionization mass spectrometry,[54] and 3.01 eV calculated at the CASPT2(7,8)/6-31G(d,p)//B3LYP/6-311++G(d,p) level of theory.[55] In good agreement with these values, analysis of the CID data yields a 0 K dissociation energy for CO loss from phenol cation of 3.03 ± 0.14 eV.[52] Significantly, the energy dependent $k(E)$ rates used to reproduce the kinetic shift in the CID data also reproduce the PEPICO rates of dissociation as a function of photon energy.

More commonly, dissociations of ionic molecules involve loose TSs, generally in the orbiting limit, especially for ion−molecule complexes that are electrostatically bound by ion−dipole attractions or hydrogen bonding. In this case, $E_R^\dagger(J)$ is equated to the height of the centrifugal barrier, $V_{eff}(r^*)$, above the asymptotic energy of the products. For the central ion−induced-dipole interaction, $V_{eff}(r) = \alpha e^2/8\pi\varepsilon_0 r^4 + L^2/2\mu r^2$ where α, e, ε_0, r, L, and μ are defined above. Assuming that the 2D angular momentum is adiabatic, L can be equated with the rotational angular momentum of the EM, which can be shown to give the height of the centrifugal barrier as

$$E_R^\dagger(J) = V_{eff}(r^*) = (\pi\varepsilon_0/2\alpha e^2\mu^2)(\hbar^2 E_R(J)/hcB)^2 \quad (13)$$

The derivation of this equation is described in detail elsewhere.[39,44] This expression is used in eq 11, and its distribution is determined by the statistical distribution of $E_R(J)$ in eq 12. Clearly, this approach makes the TS product-like (orbiting or PSL TS) and specified by the properties of the products, α and μ, and of the EM, $E_R(J)$ and B. Furthermore, this approach is variational in nature as the location of the TS changes with J. The use of PSL TSs has been found to be appropriate for a wide range of loosely bound ion−molecule complexes with electrostatic (noncovalent) type of bonding.[32,44,56−59]

Extensions of this approach that consider the influence of a permanent dipole moment on the long-range ion−molecule potential have also been described.[60] For the $K^+(NH_3)_x$ systems examined in this work, it was found that the influence of including the dipole on the data analysis changed the thresholds determined by less than 0.02 eV. For CID of proton-bound dimer anions,[61] inclusion of the permanent dipole (in the locked-dipole approximation) made a larger difference (up to 0.1 eV) in absolute thresholds, but the deviation was much smaller (<0.03 eV) for the relative threshold energies of the two product channels.

A cautionary study regarding the character of loose TSs involves the decomposition of *o*- and *p*-dichlorobenzene, *o*,*p*-$C_6H_4Cl_2^+ \rightarrow C_6H_4Cl^+ + Cl$, a simple bond fission reaction with no barrier in excess of the product asymptotic energy.[62] In this system, molecular parameters appropriate for a PSL TS do not reproduce PEPICO rates of dissociation. Rather a tighter TS is required and identified using ab initio theory. The failure of the PSL approach in this case can be rationalized by the fact that the covalent C−Cl bond involves a much stronger interaction than noncovalent interactions, yielding a tighter TS. Indeed, calculations of the potential energy for dissociation of dichlorobenzene cation deviate strongly from the ion−induced-dipole interaction potential assumed to be effective for the PSL TS model. Other examples of the use of a tighter TS include those for transition metal clusters,[46−49,63] where again the bonding is much stronger than noncovalent interactions. In general, the nature of the TS model must be based on knowledge of the potential energy surface for the reaction of interest, and uncertainties in the TS parameters should be included in the error analyses.

Competitive Dissociations. One of the advantages of eq 9 is that complexities in the dissociation process can be introduced easily. For example, if the ABC^+ molecule dissociates by two parallel pathways, reactions 14,

$$ABC^+ \rightarrow AB^+ + C \quad (14a)$$

$$\rightarrow A + BC^+ \quad (14b)$$

the form of the dissociation probability, $P_D(\varepsilon)$, remains the same but now the rate constant, $k(E^*,J)$, includes both pathways. In general, $k(E^*,J) = \Sigma\, k_j(E^*,J)$ for parallel dissociation pathways denoted by j, where each pathway has its own TS parameters, i.e.,

$$k_j(E^*,J) = d_j N_{vr,j}^\dagger (E^* - E_{R,j}^\dagger(J) - E_{0,j})/h\rho_{vr}(E^* - E_R(J)) \quad (15)$$

Thus, the dissociation probability for a specific channel is simply $P_{D,j}(\varepsilon) = P_D(\varepsilon) \times k_j(E^*,J)/k(E^*,J)$. In all cases, the competition between channels is handled statistically and can include both loose and tight TSs. Because the same EM is used for both pathways, statistical methods to handle competitive dissociations are straightforward to apply, as outlined in detail elsewhere.[64]

Figure 4 illustrates the application of these methods to the dissociation of the $(H_2O)Li^+(C_2H_5OH)$ complex.[64] The relative

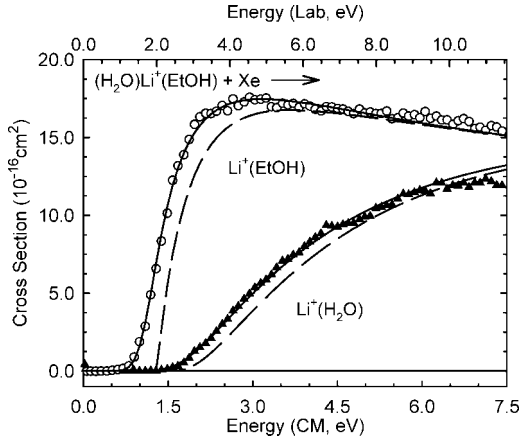

Figure 4. Cross sections for collision-induced dissociation by Xe of $(H_2O)Li^+(C_2H_5OH)$ complexes in the threshold region as a function of kinetic energy in the center-of-mass frame (lower *x* axis) and the laboratory frame (upper *x* axis). Solid lines show the best fits to the data using the model of eqs 9 and 15 convoluted over the neutral and ion kinetic and internal energy distributions. Dashed lines show the model cross sections in the absence of experimental kinetic energy broadening for reactants with an internal energy of 0 K. Reprinted with permission from ref 64. Copyright 1998, American Institute of Physics.

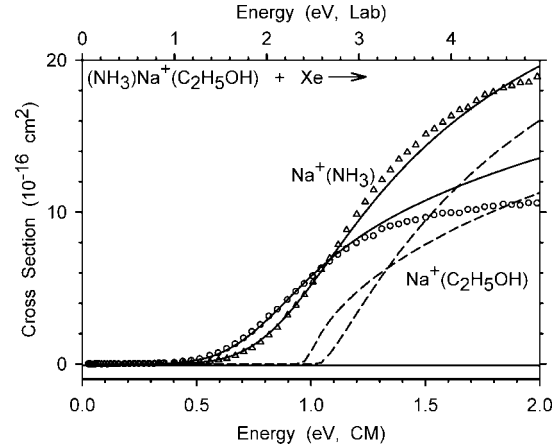

Figure 5. Zero pressure extrapolated cross sections for the competitive collision-induced dissociation of $(NH_3)Na^+(C_2H_5OH)$ with xenon in the threshold region as a function of kinetic energy in the center-of-mass frame (lower *x*-axis) and laboratory frame (upper *x*-axis). Solid lines show the best fits to the data using the model of eqs 9 and 15 convoluted over the neutral and ion kinetic energies and the internal energies of the reactants using no scaling factors. Dashed lines show the model cross-sections in the absence of experimental energy broadening for reactants with an internal energy of 0 K. The internal rotors of the ethanol in the $Na^+(NH_3) + C_2H_5OH$ channel are treated as methyl and hydroxy hindered rotors. Adapted from ref 68.

binding energies of water and ethanol to Li^+ are properly shown by the thresholds and the competition between the channels is evident by the decline in the cross section for the lower-energy $Li^+(C_2H_5OH)$ product. It can be seen that the statistical analysis reproduces this competition with fidelity and the work demonstrates that accurate relative thresholds are obtained. In this study, as well as others,[65−67] empirical adjustments of the relative magnitudes of the two channels were permitted, as these can correct for unknown factors influencing the dissociation rates.

Subsequent work[61,68] has shown that some of these empirical adjustments can be eliminated by proper consideration of nonharmonic effects. The simplest calculation of the sum and density of states in the RRKM expression, eqs 10, 11, and 15, uses the rigid-rotor, independent harmonic-oscillators approximation. However, the Beyer−Swinehart−Stein−Rabinovitch algorithms[36−39] permit efficient calculation of the sums and densities of states with nonharmonic vibrational modes, including free or hindered internal rotors. In the orbiting or PSL TS model, the relative orientational motions of the two incipient fragments are treated as free rotor modes. Anharmonic stretching vibrations can be modeled with Morse oscillator energy levels,[61] for example. Such corrections tend to have small impact for high-frequency vibrational modes, because even at the relatively high internal excitation of the EM above the dissociation threshold, the majority of these vibrational modes are populated in low vibrational energy levels, especially for larger molecules. In contrast, for low-frequency modes both the absolute frequency value and nonharmonic energy levels can have a significant impact on the densities of states. This is especially true for internal rotors with low barriers, for which symmetry effects are also often important. Figure 5 illustrates this for the case of the $(NH_3)Na^+(C_2H_5OH)$ complex, where the competition between loss of the two ligands can be accurately reproduced with no empirical scaling factors if the internal rotors of the ethanol in the $Na^+(NH_3) + C_2H_5OH$ channel are treated as methyl and hydroxy hindered rotors.[68] A key factor in reproducing these data is including the 3-fold degeneracy of the internal methyl rotor, which thereby enhances the statistical probability of this channel compared to formation of $Na^+(C_2H_5OH) + NH_3$. (The 3-fold rotational degeneracy of both NH_3 and $Na^+(NH_3)$ are also included but cancel for the two product channels.) Thus, even though formation of $Na^+(C_2H_5OH)$ is favored thermodynamically (lower threshold energy), formation of $Na^+(NH_3)$ dominates at elevated energies. It might be noted that such observations have implications for the use of the "kinetic method" for determining thermodynamics.[69,70] The basis of this method is that the relative magnitudes of competitive dissociation channels properly reflects the relative energetics of these channels, a result that the data in Figure 5 clearly belies, as discussed elsewhere.[71] Likewise, recent studies suggest that the empirical scaling factors may account for cases where vibrational frequencies (especially the low frequencies not adequately predicted by standard ab initio codes) are inaccurate by as little as 10%.

These methods are also suitable for competition between channels having both loose and tight TSs. *n*-Butylbenzene is known to dissociate by loss of propene forming $C_7H_8^+$, and at higher energies, by C−C bond cleavage to eliminate *n*-propyl, forming $C_7H_7^+$. Competitive analysis of the CID cross sections for these processes yields good agreement with literature thermochemistry when suitable TSs are located.[72] For propene loss, this is a tight TS located via theory, and for *n*-propyl loss, the best TS was again identified by utilization of PEPICO rates. This study concluded that for situations like the covalent bond cleavage associated with *n*-propyl loss, if dissociation rates were not available (the usual case), a reasonable TS could be determined as the transient structure situated at the minimum separation between the two products where the interaction energies start to be reproduced by an ion−induced-dipole model. Distances between the heavy atoms of the bond to be broken should be used instead of distances between the centers of mass of the two products. A more complicated (three channel) example finds that dissociation of the $[OCS\cdot C_2H_2]^+$ system into $OCS^+ + C_2H_2$ and $C_2H_2^+ + OCS$ via loose TSs and into $C_2H_2S^+ + CO$ via a tight TS can be accurately modeled using these statistical methods.[73] The CID thresholds are within experimental error of all known thermochemical values and are consistent with limits set by previous photodissociation[74] and KERD measurements[75] on the $[OCS\cdot C_2H_2]^+$ system.

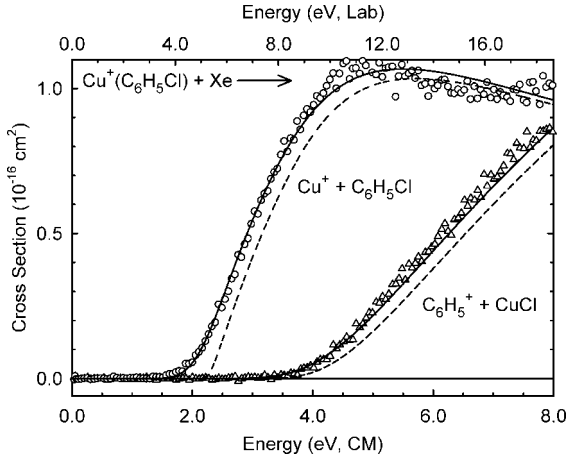

Figure 6. Zero-pressure-extrapolated cross sections for collision-induced dissociation of $Cu^+(C_6H_5Cl)$ complexes with Xe in the threshold region as a function of kinetic energy in the center-of-mass frame (lower *x*-axis) and laboratory frame (upper *x*-axis). Solid lines show the best fits to the data using the competitive model of eqs 9 and 15 convoluted over the neutral and ion kinetic and internal energy distributions. Dashed lines show the model cross sections in the absence of experimental kinetic energy broadening for reactants with an internal energy corresponding to 0 K. Adapted from ref 76.

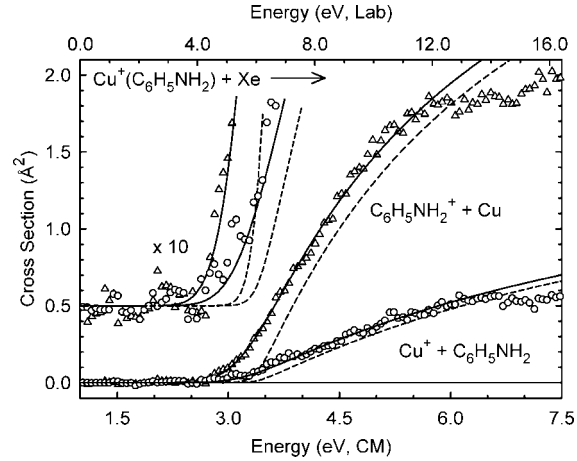

Figure 7. Zero-pressure-extrapolated cross sections for collision-induced dissociation of $Cu^+(C_6H_5NH_2)$ complexes with Xe in the threshold region as a function of kinetic energy in the center-of-mass frame (lower *x*-axis) and laboratory frame (upper *x*-axis). Solid lines show the best fits to the data using the competitive model of eqs 9 and 15 convoluted over the neutral and ion kinetic and internal energy distributions. Dashed lines show the model cross sections in the absence of experimental kinetic energy broadening for reactants with an internal energy corresponding to 0 K. Adapted from ref 76.

These statistical methods can also be used to characterize very different types of dissociation processes, as illustrated for a variety of copper-cation$-\pi$ complexes, $Cu^+(\pi\text{-ligand})$.[76] Figure 6 shows an example where two types of noncovalent bond cleavage processes compete. Here, the $Cu^+(C_6H_5Cl)$ complex dissociates to produce Cu^+ and C_6H_5Cl as well as $C_6H_5^+$ and CuCl. As a result of the ionic character of the transition states for both dissociation pathways, these data are accurately reproduced using loose PSL TSs for both dissociation channels with no need for adjustments to the relative magnitudes of the two channels. Similar results are found for the $Cu^+(C_6H_5Br)$ and $Cu^+(C_6H_5I)$ systems, where the relative differences in the energy thresholds for the two product channels become smaller such that the $C_6H_5^+$ channel becomes increasingly favorable. An additional higher energy dissociation channel is also available to the $Cu^+(C_6H_5I)$ system, resulting in cleavage of the C$-$I bond to produce $Cu^+(C_6H_5)$ and I. In this latter case, all three product cross sections can be accurately reproduced using loose PSL TSs.

A second type of competition is illustrated in Figure 7, where the $Cu^+(C_6H_5NH_2)$ complex dissociates by simple noncovalent bond cleavage to produce either $Cu^+ + C_6H_5NH_2$ or $C_6H_5NH_2^+ + Cu$. These charge transfer channels clearly compete as a result of the similar ionization energies of Cu and $C_6H_5NH_2$. Again, these data are accurately reproduced using loose PSL TSs for both dissociation channels. Similar competition between products differing only in charge state has been observed for $Cu^+(C_8H_7N)$, $Cu^+(C_4H_4NCH_3)$, and $Cu^+(C_6H_5NHCH_3)$ systems[76] as well as for the Zn^+(imidazole) complex.[77]

Ligand Exchange. The influence of competition on reaction probabilities can also be directly observed in ligand exchange processes, the forward and reverse directions of reaction 16.

$$AB^+ + C \leftrightarrow BC^+ + A \quad (16)$$

In such a reaction, the transient intermediate formed, ABC^+, is the same chemical species interrogated by CID in reaction 14. An example is shown in Figure 8 for reaction 17

$$Na^+(CH_3OH) + NH_3 \rightarrow Na^+(NH_3) + CH_3OH \quad (17a)$$

and its reverse (where deuterated ammonia is needed for mass separation purposes).

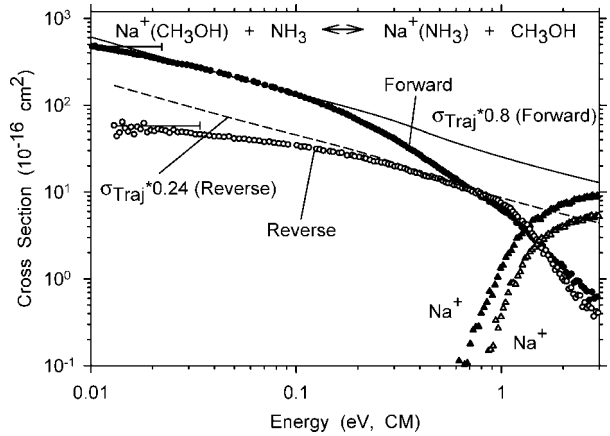

Figure 8. Zero-pressure-extrapolated cross sections for the reactions of $Na^+(CH_3OH)$ with NH_3 (solid symbols) and $Na^+(ND_3)$ with CH_3OH (open symbols) as a function of kinetic energy in the center-of-mass frame. ($Na^+(ND_3)$ is used as the reagent in the latter reaction rather than $Na^+(NH_3)$ to resolve it from the isobaric Ar^+ ion also present in the source.) Solid and dashed lines display the theoretical collision cross sections, σ_{Traj}, for the forward and reverse reactions, respectively, multiplied by an arbitrary scaling factor to bring its magnitude into agreement with the data. Uncertainties in the absolute energies are shown for the lowest-energy cross section data point for the ligand exchange reactions. Adapted from ref 78.

$$Na^+(ND_3) + CH_3OH \rightarrow Na^+(CH_3OH) + ND_3 \quad (17b)$$

Here the forward reaction is exothermic and hence the cross section is much larger than the reverse endothermic process.[78] It can be seen that the exothermic, forward process has a measured cross section with an energy dependence in good agreement with the predicted collision cross section, σ_{Traj},[79] but the magnitude is smaller (80%). For the endothermic, reverse cross section, the magnitude is smaller (24% of σ_{Traj}) and deviates from this prediction at the lowest energies because of the endothermicity. In this system and several others, endothermicities obtained by analyzing the endothermic cross section using eq 9 were found to be systematically higher than literature values because these thresholds are shifted by competition with the thermoneutral reaction back to reactants.[68] However, if

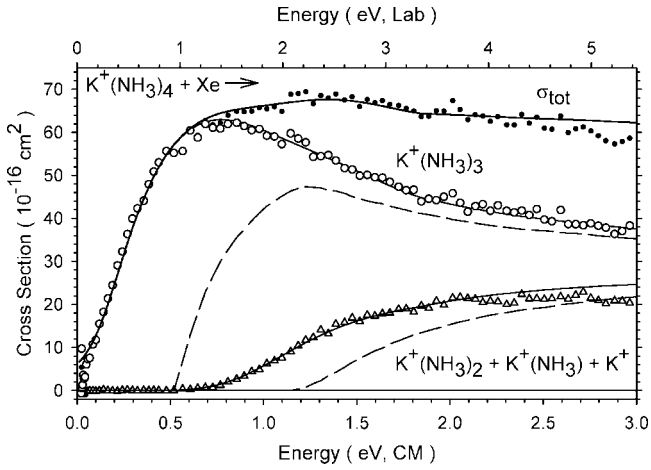

Figure 9. Zero pressure extrapolated cross sections for collision-induced dissociation of $K^+(NH_3)_4$ with Xe in the threshold region as a function of kinetic energy in the center-of-mass frame (lower *x*-axis) and the laboratory frame (upper *x*-axis). Solid lines show the best fit to the primary and secondary product cross sections using the model of eq 19 convoluted over the neutral and ion kinetic and internal energy distributions. Dashed lines show the model cross sections in the absence of experimental kinetic energy broadening for reactions with an internal energy of 0 K. Reprinted with permission from ref 81. Copyright 2007, American Institute of Physics.

statistical methods are used to include this competition, literature endothermicities are reproduced. Likewise, this procedure can be used to reproduce the absolute magnitudes of the exothermic ligand exchange cross sections, which are reduced from 100% efficiency by competition with the thermoneutral reaction back to reactants. The magnitudes depend critically on the exothermicities and are reproduced well when exothermicities used in the modeling are in agreement with literature values.[78]

Ligand exchange reactions examined in both directions can also be used to provide free energies of reaction.[78] Combining these with reaction enthalpies can then be used to yield dissociation entropies that agree well with both experimental[80] and theoretical entropies[59,68] available in the literature. For $Na^+(C_2H_5OH)$, the best agreement between the experimental and theoretical entropies was obtained when the methyl and hydroxyl internal torsions were treated as vibrators in the complex and hindered rotors in the neutral product, the same treatment noted above in the competitive CID results shown in Figure 5.

Sequential Dissociations. A statistical approach also allows straightforward extension to sequential dissociation processes, reaction 18.

$$ABC^+ \rightarrow AB^+ + C \rightarrow A + B^+ + C \qquad (18)$$

Once the cross section for the first dissociation process is determined using eq 9, the probability for a secondary dissociation, $P_{D_2} = \langle 1 - e^{-k_2(E_2^*,J_2)\tau_2} \rangle$, is included as in eqs 19.[81]

$$\sigma(E,AB^+) = (\sigma_0 n/E)\sum_i g_i \int_{E_0-E_i}^{E} P_{D1}(1 - P_{D2})(E-\varepsilon)^{n-1}\, d\varepsilon \qquad (19a)$$

$$\sigma(E,B^+) = (\sigma_0 n/E)\sum_i g_i \int_{E_0-E_i}^{E} P_{D1}P_{D2}(E-\varepsilon)^{n-1}\, d\varepsilon \qquad (19b)$$

This partitions the total CID cross section into the cross section for those primary products, AB^+, that do not dissociate, $\sigma(AB^+)$, and those that do, $\sigma(B^+)$. Subsequent dissociation may not occur because the primary AB^+ products have either insufficient energy or time. The key problem in calculating P_{D_2} is determining the values of E_2^* and J_2. In the first dissociation, the energy available to the products, $E_1^* = \varepsilon + E_i - E_0$, can be distributed into relative translation of the products, and internal energy of the two fragments, but only the internal energy left in AB^+, E_2^*, is available for further dissociation. In the orbiting or PSL limit, the TS is product-like and statistical assumptions become a powerful means of determining how this energy is distributed among these degrees of freedom. For tight TSs, additional assumptions would need to be made as the reverse activation energy can be released nonstatistically into the available degrees of freedom. It should also be realized that because of the treatment of the orbital angular momentum at the TS (see above), some of the rotational energy of the EM is assumed to be directed into relative translation motion. The means, to estimate, E_2^* and J_2 have been outlined elsewhere in detail.[81] In principle, these methods can be applied iteratively for further sequential dissociations, but keeping track of the various distributions becomes intractable in practice.

Figure 9 illustrates the utility of this procedure for the example of the $K^+(NH_3)_4$ complex. It can be seen that the shapes of both cross sections (as well as the total cross section) are well reproduced. Further, the bond energies obtained for $D_0[(NH_3)_3K^+-NH_3]$ and $D_0[(NH_3)_2K^+-NH_3]$ agree well with independent measurements.[60,82] As for competitive dissociation, an empirical scaling factor is needed to accurately reproduce the relative magnitudes of the data. This is likely a consequence that the statistical procedure outlined above does not rigorously conserve angular momentum, but further studies are needed to verify this suggestion. Nevertheless, this statistical approach does provide an accurate assessment of the energy dependence of the cross sections, which is what is needed for thermodynamic measurements.

Association. The assumptions concerning angular momentum effects were explored more sensitively by examining the reverse of the CID dissociation process 2b, i.e., association, reaction 20.[83]

$$AB^+ + C \rightarrow ABC^+ \qquad (20)$$

The bimolecular association reaction allows the energized molecule ABC^{+*} to be formed under conditions in which the internal energy (E^*) and rotational angular momentum distributions (J) are well characterized. Under collisionless conditions, this EM can either dissociate back to reactants or be observed if its lifetime is longer than the detection time window. By varying the kinetic energy of the reactants, the internal energy and thus the lifetime can be systematically varied. The kinetic energy dependences of the cross sections for association of $M^+ = Li^+$, Na^+, and K^+ with dimethoxyethane (DXE) were determined as a function of the pressure of DXE and extrapolated to single collision conditions to avoid contributions of collisional deactivation to formation of the M^+(DXE) complexes.[83] The results were interpreted using several different models, including phase space theory in which angular momentum is rigorously conserved. In these models, the only adjustable parameter is the M^+-DXE bond energy, previously measured using CID methods.[84−86] In all cases, the TS was assumed to be a loose, orbiting PSL TS. Even though the models had very different assumed rotational energy distributions, the

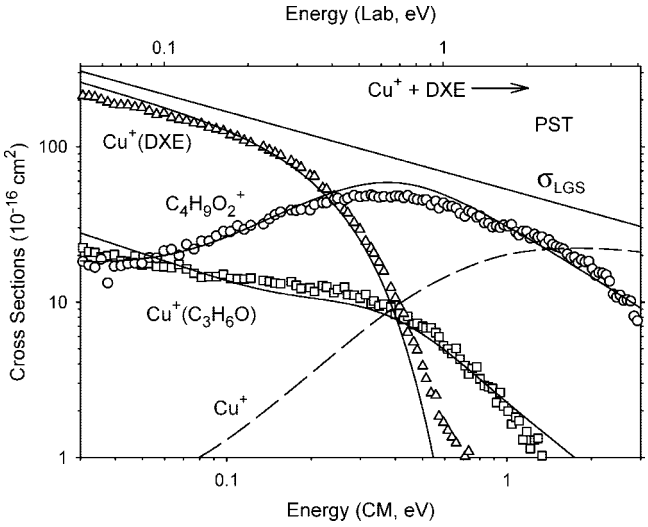

Figure 10. Comparisons of the experimental data with a statistical model for the reaction of Cu^+ with $(CH_3OCH_2)_2$ (DXE) as a function of kinetic energy in the center-of-mass frame (lower *x*-axis) and laboratory frame (upper *x*-axis). Points indicate zero pressure extrapolated cross sections for three channels, Cu^+(DXE), ($C_4H_9O_2^+$ + $C_3H_7O^+$) and $Cu^+(C_3H_6O)$. Solid lines show the best fit to the three channels using a phase space theory (PST) model. The dashed line indicates the model cross section for the Cu^+ + DXE dark channel (back to reactants). The LGS collision cross section is also indicated. Reprinted with permission from ref 87. Copyright 2004, American Institute of Physics.

binding energies required to reproduce the data varied little and were self-consistent with the values measured using CID.

A more sensitive test was provided by the association reaction of Cu^+ with DXE.[87] Here, simple association to form Cu^+(DXE) competes with two lower energy reactive processes, formation of $C_4H_9O_2^+$ + CuH (where the product ion dissociates into $C_3H_7O^+$ at higher energies) and of $Cu^+(C_3H_6O)$ + CH_3OH. Again the use of several models involving different assumptions about the rotational energy distributions shows that reproduction of the cross sections for the two channels involving loose TSs, Cu^+(DXE) and $C_4H_9O_2^+$, is not particularly sensitive to these assumptions, whereas the cross section for $Cu^+(C_3H_6O)$, which involves a tight TS, is reproduced well only when the correct angular momentum distribution available to the energized Cu^+(DXE) molecule is considered, Figure 10. However, the thermochemistry obtained from these analyses is less sensitive to the assumptions made, in that all models reproduce the previous results obtained from CID studies.[88] Even so, the best thermodynamic results again appear to be obtained for the correct angular momentum distribution.

These association reactions provide a powerful means of determining thermochemistry for systems for which the lifetimes for dissociation are large. In a CID process, long lifetimes lead to extensive kinetic shifts such that the extrapolation from the apparent CID threshold energy to the true thermodynamic threshold can be large. Because of the uncertainties associated with the energy deposition function and the true angular momentum distribution of collisionally activated molecules, such large extrapolations may lead to large uncertainties in the extracted threshold energies. In contrast, association avoids many of the unknown distributions and takes advantage of the long lifetimes of the species.

Surface-Induced Dissocation. Although beyond the main focus of this work on gas-phase processes, it is noteworthy that statistical rate theory has also been profitably applied to kinetic energy-resolved dissociation of ions upon impact with surfaces.[89,90] For surface-induced dissociation (SID), the collisional energy transfer distribution function is found to be similar to a thermal distribution, but with an effective temperature that is not directly proportional to the collision energy.[89] The energy transfer efficiencies have been shown to vary with the type of surface used.[91] Similar issues of kinetic and competitive shifts apply for both SID and CID.

Implementation. Octopole guided ion beam tandem mass spectrometers have been developed in our laboratories[23,63,92,93] with designs optimized for accurate measurement of reaction cross sections with well-defined ion kinetic energies. Key design considerations include (1) an ion source that produces ions with a thermalized ion population at a known internal temperature and narrow kinetic energy distribution; (2) a magnetic sector initial mass spectrometer and ion focusing and acceleration/deceleration optics to produce a well-collimated ion beam; (3) the radio frequency ion beam guide for near-4π collection of scattered product ions and operation over a wide range of ion energies (routinely from room temperature up to accelerating potentials of 1000 V); (4) a gas collision cell with a well-defined length and pressure; (5) an analysis quadrupole mass filter with a broad angular and energy ion acceptance aperture and unit mass resolution; and (6) pulse-counting ion detector with high detection efficiency. Although commercial triple quadrupole mass spectrometers, which utilize an rf-only quadrupole reaction region, can be adapted for kinetic energy dependent cross section measurements, using a quadrupole for the initial mass filter tends to perturb the ion energy distributions and the reaction region is not well-defined in either length or energy. Use of such instruments often produces artifact "tails" in the threshold region because of nonuniform ion energy distributions.[94−99]

The statistical rate theory models described here, as well as convolutions over kinetic energy distributions have been implemented in CRUNCH, a Fortran program available from the authors for general analysis of cross sections as a function of kinetic energy. Many of the transition-state theory formalisms and some underlying code are derived from the work of Chesnavich, Bowers, and their co-workers.[12−18] The various integrations involved in evaluating eqs 7−9 are carried out numerically, with storage of intermediate values of partial integrands and distribution functions allowing very efficient calculations. The current version of CRUNCH can model molecules with up to 256 vibrational modes but can readily be recompiled for larger molecules. Others have independently implemented energy-resolved cross section analysis methods including statistical rate theory models,[100,101] some using Monte Carlo integration methods[102−104] or approximate empirical formulas for the density of state functions.[102]

Applications

Metal−Ligand Systems. As noted above, the use of statistical methods to analyze CID thresholds extends the dynamic range of such experiments from small, weakly bound systems to much larger and strongly bound systems. For example, alkali metal cation complexes with single ligands ranging in BDE from 33 kJ/mol for Li^+(Ar) to 372 kJ/mol for Li^+(12-crown-4), 15 kJ/mol for Na^+(Ar) to 296 kJ/mol

for Na^+(18-crown-6), and 14 kJ/mol for K^+(Ar) to 235 kJ/mol for K^+(18-crown-6) have been reported, as well as smaller sets of data for Rb^+ and Cs^+ complexes.[50] Similar ranges have been explored for both singly charged alkaline earth and transition metal complexes as well by our groups,[50,105,106] and for silver cations by Siu and co-workers.[107−109] Further, there are few limitations with regard to multiple ligation. For example, these techniques have been used to measure the binding energies of lithium cations to one to six water molecules,[58] titanium and vanadium cations with one to seven carbonyl ligands,[110,111] and copper cations with six methanols[112] and a number of complexes with four ligands including molecules as complicated as 4,4′-bipyridine.[113] Recent advances have demonstrated that bond energies to multiply charged ions are accurately characterized using these methods, e.g., $Ca^{2+}(H_2O)_x$, $x = 5-9$,[114] and additional experimental advances are allowing the complete inner solvent shell, $x = 1-4$, to be similarly characterized.[115] Ligands amenable to study include very simple (rare gases, carbon monoxide, water, ammonia)[50] to various biologically relevant systems including nucleobases,[116−121] amino acids,[118,122−124] sugars,[125] and phosphates.[126,127] Recently, bond energies of Na^+ and K^+ to a simple dipeptide and tripeptide were measured using these methods[128] and on the basis of crown ether studies,[50,129] it is anticipated that hexapeptides and perhaps larger peptides can be profitably studied. Furthermore, the influence of hydration on such metal−ligand interactions has been studied using these statistical methods, e.g., Na^+(glycine)$(H_2O)_x$[130] and Na^+(proline)$(H_2O)_x$ ($x = 1-4$).[131] Such studies provide a bridge to extrapolating the thermochemistry from the gas-phase to solution media.

More complex transition metal systems with complete ligand shells directly analogous to solution-phase systems have been studied using these techniques by Chen and co-workers. Such systems include C−H bond activation at Ir(III) centers,[132] as first characterized in solution by Bergman;[133,134] ligand binding to Pt(II) complexes;[135,136] dissociation of a rhenium diolate complex by rearrangement to the cyclic rhenaoxetane, which dissociates by [2 + 2] scission to form a metallocarbene and aldehyde;[137] and 2:1 complexes of bis(oxazoline) and azabis(oxazoline) ligands with Cu(I), useful as asymmetric catalysts.[138,139]

The extensive range of the experimental data has enabled comprehensive comparisons of experimentally determined bond energies to those of theory over an extended range. For example, seventeen sodium cation complexes ranging in BDE from 15 kJ/mol for Na^+(Ar) to 158 kJ/mol for $Na^+(CH_2OCH_3)_2$ were compared to several levels of theory.[59] Calculations at the CBS-Q,[140] B3P86/6-311+G(2d,2p)//B3P86/6-31G(d), and MP2(full)/6-311+G(2d,2p)//MP2(full)/6-31G(d) levels of theory were found to reproduce the results well, within about 5 kJ/mol. Hoyau et al. reached the same conclusion regarding the latter level of theory using a smaller set of experimental BDEs.[80] In contrast, the popular B3LYP approach is systematically high by about 8 kJ/mol. In the case of lithium cation complexes, such a comparison suggests that basis sets that include core correlation on the lithium cation (as designated by Li−C) are needed to provide the best theoretical numbers.[141] Complete basis set extrapolations are found to provide the most accurate thermochemistry, but the MP2(full)/aug-cc-pVTZ(Li−C)//MP2(full)/cc-pVDZ(Li−C) level of theory excluding corrections for basis set superposition errors provides a good reproduction of the data as well.

Metal Clusters and Adsorbates. As noted above, these methods have been applied to a host of systems involving transition metal clusters. Early work focused on measurements of the BDEs of bare transition metal cluster cations by CID studies.[48,142] Combined with ionization energy measurements of the bare clusters, this also enables the determination of the BDEs for *neutral* transition metal clusters. More recent efforts have expanded to include studies of bimolecular reactions with species such as H_2, O_2, N_2, CO_2, CH_4, and NH_3 (or deuterated variants).[143,144] This enables the measurement of the binding energies of adsorbates such as H, C, N, O, CH_x, and NH_x ($x = 1 - 3$) to transition metal cluster cations. These studies have demonstrated the surprising result that such adsorbate BDEs reach an asymptotic level at relatively small cluster sizes, about 10 atoms, and furthermore that this asymptotic level matches binding energies on surfaces in cases where such data are available (primarily H and O). Ongoing work includes studies of metal oxide clusters with varying stoichiometry, as also studied using these methods by Castleman and co-workers.[145]

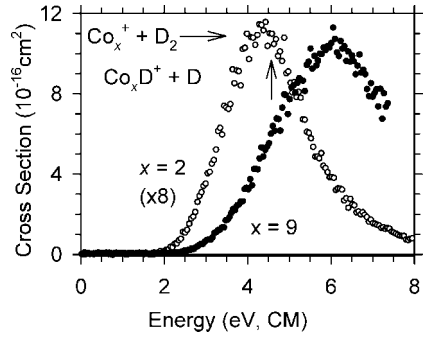

Figure 11. Cross sections for reactions of Co_2^+ (open symbols) and Co_9^+ (solid symbols) with D_2 as a function of collision energy in the center-of-mass (lower *x*-axis) and laboratory (upper *x*-axis) frames. The bond energy of D_2 is indicated by the vertical arrow at 4.56 eV. Data taken from ref 146.

These bimolecular reactions provide an obvious demonstration of the presence of kinetic shifts, as shown in Figure 11, which shows the cross sections for reactions of cobalt cluster cations, Co_x^+, with D_2 to form $Co_xD^+ + D$.[146] The cross sections for these reactions reach a maximum because the product can dissociate in the overall reaction, $Co_x^+ + D_2 \rightarrow Co_x^+ + D + D$, which has a thermodynamic onset equivalent to $D_0(D_2) = 4.56$ eV. It can be seen that the cross section for $x = 2$ peaks at this energy, as expected, whereas that for $x = 9$ is shifted to higher energies. Indeed, it is found that the peak systematically shifts to higher energies as the size of the cluster cation increases (not only for cobalt but also for other metal clusters).[147−150]

Ervin and co-workers have used energy-resolved CID and time-resolved photodissociation, both modeled by RRKM theory, to measure the binding energies of anionic transition metal clusters and of ligands bounds to the clusters.[151−156] In the case of CO ligands binding to group 10 clusters, different binding sites could be identified by distinct dissociation energies as a function of the number of CO ligands.[152,154] Because mass spectrometry does not provide direct structural information, the geometries of the binding sites must be inferred. For example, the first three carbonyls on triangular Pt_3 clusters have strong bonds and the next three have relatively weak bonds. On the basis of molecular orbital arguments including the expected relative effectiveness of π-back-bonding for bridged (edge) and terminal (atop) sites, it was argued that the first three CO ligands bind at bridged sites and the next three at terminal sites.[152,154] A decade later, density functional theory calculations for heavy metals became sufficiently advanced to show that this geometry

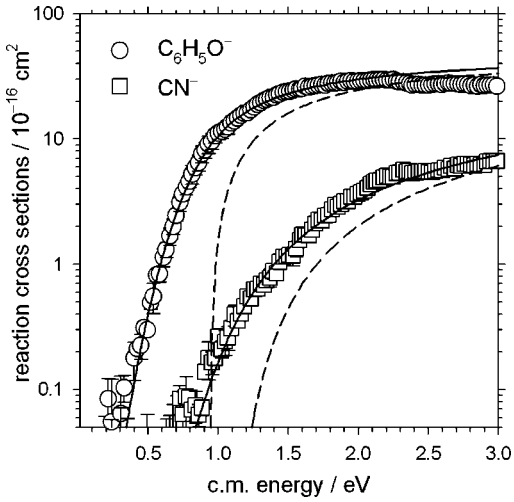

Figure 12. Single-collision TCID cross sections for $[C_6H_5O{\cdot}H{\cdot}CN]^- \rightarrow C_6H_5O^- + HCN$, $CN^- + C_6H_5OH$ as a function of relative collision energy between $[C_6H_5O{\cdot}H{\cdot}CN]^-$ and Xe. Solid lines show the convoluted fits to the data and dashed lines the corresponding unconvoluted 0 K model cross sections. Adapted from ref 173.

assignment was reversed; the calculations actually show that relativistic effects in platinum favor the terminal sites over bridged sites.[157]

In the case of photoactivation of silver and gold cluster anions,[158,159] it was found that photodissociation competes with two distinct electron-loss processes: direct photodetachment and delayed thermionic emission. The competition between unimolecular dissociation and delayed electron emission was modeled as a statistical process, assuming the vibronic degrees of freedom are coupled. Shvartsburg et al.[160,161] discussed theoretically the application of RRKM theory to metal cluster systems with many low-lying electronic states, another situation where vibronic coupling may be important.

Proton-Bound Clusters. In addition to the metal-based systems described above, the statistical methods discussed here have been used to study proton bound complexes, both cationic and anionic. For instance, the Armentrout group has examined the CID behavior of protonated water clusters, $H_3O^+(H_2O)_x$, $x = 1-5$,[162] and obtained sequential solvation enthalpies in excellent agreement with values obtained from equilibrium measurements.[163−166] Later measurements extend the application of these methods to hydrogen/deuterium exchange reactions of $H_3O^+(H_2O)_x + D_2O$ and $D_3O^+(D_2O)_x + H_2O$ ($x = 1 - 3$).[167] Here, RRKM calculations of the isomerization and dissociation rate constants accurately predict the observed branching fractions and allow measurement of the energy of the rate-limiting step needed for H/D exchange, a four-centered transition state also identified by ab initio calculations. More recently, these methods have been used to explore the dissociation of protonated species including: indole, amino acids and small peptides.[94,168−171] Such studies enable the accurate measurement of the energies of transition states for decomposition of these species, and thus a positive identification of the mechanisms involved.

The relative gas-phase acidities of two molecules can be determined by competitive CID of a proton-bound dimer anion of the corresponding conjugate bases.[172] In a recent example, the gas-phase acidity of phenol (C_6H_5OH) and several cresols (methyl-substituted phenols) were determined by CID of their complexes with CN^-, HS^-, and O_2^-, i.e., using HCN, H_2S and HO_2 as reference acids.[173] Figure 12 shows the CID cross sections for $[C_6H_5O{\cdot}H{\cdot}CN]^-$, for example. The C_6H_5O-H bond dissociation energy derived from the measured acidity is $D_0 = 356 \pm 4$ kJ/mol,[173] which agrees with a subsequently published photofragment translational spectroscopy value, $D_0 = 359.1 \pm 0.5$ kJ/mol,[174] which settles a long controversy. There are two advantages of the competitive CID method over traditional equilibrium acidity measurements by high-pressure or ion cyclotron mass spectrometry. (1) Because of the large collision energy range in threshold CID (TCID), the acidities of the unknown and acid can be farther apart for TCID (up to about 50 kJ/mol) than in most thermal equilibrium measurements. (2) The pressures of the neutral acids do not need to be determined, which means nonvolatile or reactive (e.g., HO_2 above) species can be used as long as the ion complexes can be formed. Although the need to model the cross sections using statistical rate theory is a disadvantage compared with direct equilbrium measurements, the product branching fractions are very sensitive to the relative acidity. Consequently, experimental and modeling errors tend to cancel when determining an energy difference rather than an absolute threshold energy.

Determining relative gas-phase acidities (or other ion affinities) by competitive CID methods is robust because the relative energy measurement depends on modeling the branching fractions of two similar product channels with statistical rate theory, rather than extrapolating to an absolute threshold energy by modeling the kinetic shift. Comparisons of RRKM theory versus PST and of various treatments of the long-range ion−dipole potential have shown weak sensitivity of the obtained relative acidities to these modeling choices.[175,176]

Covalent Molecular Ions. A host of covalently bound systems can also be examined using these statistical methods. Several examples, e.g., dissociation of the cations of phenol,[52] dichlorobenzene,[62] and *n*-butylbenzene,[72] were noted above, but many other types of systems are amenable to study as well. For instance, as originally implemented by Wenthold and Squires,[96] energy-resolved CID analyzed using the statistical methods outlined here has been used to measure thermochemistry for a wide range of reactive organic species. Recent studies include isonitrile (HNC),[177] diradicals such as cyanocarbene (HCCN),[178] methylhydroxy carbene,[179] *m*-xylylene,[97] and triradicals such as 1,3,5-tridehydrobenzene[180] and 1,3,5-trimethylene benzene.[181] Sunderlin and co-workers have used CID techniques to measure bond energies of halide anions to other halogens,[98,182] to phosphorus,[183,184] to chalcogenides (S, Se, Te) and chalcogenide oxides,[185−187] to Si, Ge, and Sn tetrahalides and dimethyl dihalides,[188] and in rare gas compounds such as XeF_3^-.[99] Wenthold and co-workers have used CID and reactivity studies of $Al_2H_7^-$ to measure the bond energy of the dialane molecule, $(AlH_3)_2$.[189]

Current Challenges. Despite the success of statistical methods in describing the complex behavior of kinetic energy dependent dissociation experiments, our previous efforts point out several types of systems that challenge the current modeling methods. As noted above, it is always possible for a system to behave nonstatistically and this possibility becomes more likely for smaller systems. Indeed, failures of this collisional approach have been documented for several diatomic systems, including several transition metal oxides (MO^+ where M = V,[190] Y, Zr, Nb, Mo,[191] and Pt[192]) and O_2^-.[193] In the metal oxide systems, the CID cross sections rise very slowly from near the thermodynamic thresholds, increasing more rapidly at higher collision energies. Such behavior indicates inefficient transfer of translational energy into internal energy at the high collision energies required to dissociate these strongly bound diatomic ions. Ultimately, such behavior can be attributed to the very strong

bonds involved, $D_0(MO^+) = 3-8$ eV, such that collisional excitation is not sufficiently adiabatic. However, such observations are not universally true, e.g., CID of SiF^+ yields a measured bond energy of 7.04 ± 0.06 eV,[194] in excellent agreement with high-level theory, 6.90 ± 0.09 eV.[195] In collision-induced dissociation of O_2^-, the threshold energies determined from experiment using eq 8 exceed the known bond dissociation energy by 2.1 and 1.1 eV for argon and xenon target gases, respectively.[193] Classical trajectory calculations show that the reaction probability is highly dependent on orientation, with only near-perpendicular approaches contributing to efficient dissociation, which results in severe kinematic constraints.[193] Obviously, nonstatistical dynamic effects cannot be treated by statistical rate theory.

A further limitation of our statistical rate modeling approach is that we use either fixed, tight transition states or loose, orbiting (PSL) transition states rather than full variational microcanonical transition-state theory,[24] which finds the minimum sum of states along the true potential energy surface for dissociation at each energy. Sawilowsky and Klippenstein[196] have examined the possibility that ion−molecule reactions exhibit both "inner" (tight TS) and "outer" (PSL TS) bottlenecks. Where such issues appear to be important because of known features along the potential energy surface, the transition-state switching model of Chesnavich et al.[197] may be used as an approximation.[61,198] In general, however, the potential energy surfaces for most systems are insufficiently well characterized for the full variational treatment to be feasible.

For larger and thus longer lived systems, radiative relaxation processes may begin to compete with dissociation. This could directly affect the energy distribution available to the energized molecule, slowing the dissociation rate and increasing the kinetic shift. For the present experiments, where the time available for dissociation is about 10^{-4} s, IR radiative rates are still too slow to be of major concern, but if such methods are to be extended to larger systems with much longer lifetimes, then such effects must eventually be incorporated into the statistical approach. Dunbar and co-workers[199] have developed models for radiative emission rates.

Another complication that becomes pervasive for larger systems, in particular of biologically relevant molecules is multiple conformations. It is clear that the dissociations of many of these types of systems involve a complex energy landscape with many different stable intermediates. The present statistical approach generally uses molecular parameters for the rate-limiting step as the transition state (TS) and for the most stable complex as the energized molecule (EM). Jia et al.[198] discussed the statistical treatment of multiple conformations of the EM for CID of proton-bound carboxylate dimer anions. In those complexes, the formation of multiple hydrogen bonds creates several low-lying conformational isomers of the complex, each of which can dissociate either directly to ground-state products or indirectly via isomerization over barriers below the dissociation energy. In this and other systems, it is possible that a dynamic equilibrium among the various stable intermediates (conformations) is established even at modest excitation energies such that the EM can access multiple conformers. If redistribution of the populations of these conformers has a rate slower than or comparable to the dissociation rate, then the presence of these other conformations will affect the dissociation rate observed. In such cases, a transition-state-switching statistical model could be applied if the isomerization barrier heights are sufficiently well-known from theory, but branching ratio data alone are not sufficient to constrain the interconformer barrier heights if they are treated as adjustable parameters.[198] A related problem, noted in the Introduction, concerns isomerization barriers of moderately large molecules. When the energy barriers to such processes are low, the isomerization rates can approach the dissociation rates. Methods developed for correcting statistical rates when IVR is limiting,[25,26] in principle, could be incorporated into the methods discussed here, although that could require theoretical estimates of the vibrational coupling parameters.

In another limit, studies have been performed on metallated molecules having tautomers separated by barriers sufficiently high that no communication between them is possible over the excitation energy ranges examined. Species included in this category include the azoles[200] and the nucleobases.[116,117,119−121] In such cases, the dissociation behavior is clearly limited to the tautomer formed experimentally, which may then dissociate to products corresponding to something other than the ground-state tautomer.

When using any thermokinetic method to obtain thermochemical information, modeling issues such as those described in this section can lead to inaccurate results if they are not identified. The energy-resolved ion beam methods described here intrinsically limit such errors because the models are constrained by the experimental data over a very broad energy range, rather than for a single temperature or a small range of temperature as is found in many other kinetics experiments. A further important means of quality control is the measurement of the same thermochemical quantity via multiple systems or pathways. For example, local thermochemical networks of relative gas-phase acidities can be used to refine and constrain absolute acidity values.[172,173,201] Comparison of experimental values with theory, as is routine in most of our work,[35,50,59,141] is also a valuable way of identifying problem cases.

Conclusion

The use of statistical rate theory to estimate the effects of kinetic shifts on collision-induced dissociation reactions has proven to be robust, allowing systems under study to be extended from relatively small systems to much larger complexes and clusters. Such larger systems exhibit appreciable kinetic shifts; however, by including a statistical estimate of these shifts, the threshold energies obtained from such CID studies provide accurate measures of the thermochemistry of the systems being interrogated. These statistical approaches can be extended to more complicated systems involving competition between parallel and sequential dissociation channels, further expanding the quantitative applicability of the approach. Likewise, association reactions and ligand exchange (equilibrium-like reactions) can be quantitatively assessed using the same general approach. Overall, the use of statistical rate theories in kinetic energy-resolved mass spectrometric measurements provides quantitative thermochemistry for a wide range of chemical systems, including metal−ligand complexes, metal clusters, proton-bound complexes, organic intermediates, biological systems, saturated organometallic complexes, and hydrated species. Further applications and extensions can be anticipated.

Acknowledgment. We thank the National Science Foundation (CHE-0748790, PBA; CHE-9816206, KME; and CHE-0518262, MTR) and the Chemical Sciences, Geosciences, and Biosciences Division, Office of Basic Energy Sciences, Department of Energy (PBA and KME) for their support of this research over the years. Many dedicated students and postdoctoral researchers are thanked for their efforts and contributions to the advances outlined here.

References and Notes

(1) Thomson, J. J. *Philos. Mag.* **1911**, *21*, 225.
(2) Rice, O. K.; Ramsperger, H. C. *J. Am. Chem. Soc.* **1927**, *49*, 1617.
(3) Rice, O. K.; Ramsperger, H. C. *J. Am. Chem. Soc.* **1928**, *50*, 617.
(4) Kassel, L. S. *J. Phys. Chem.* **1928**, *32*, 225–1065.
(5) Marcus, R. A.; Rice, O. K. *J. Phys. Colloid Chem.* **1951**, *55*, 894.
(6) Marcus, R. A. *J. Chem. Phys.* **1952**, *20*, 359.
(7) Rosenstock, H. M.; Wallenstein, M. B.; Wahrhaftig, A. L.; Eyring, H. *Proc. Nat. Acad. Sci. U.S.A.* **1952**, *38*, 667.
(8) Chupka, W. A. *J. Chem. Phys.* **1959**, *30*, 191.
(9) Lifshitz, C.; Long, F. A. *J. Chem. Phys.* **1964**, *41*, 2468.
(10) Rosenstock, H. M. *Int. J. Mass Spectrom. Ion Phys* **1976**, *20*, 139.
(11) Baer, T.; Hase, W. L. *Unimolecular Reaction Dynamics: Theory and Experiments*; Oxford: New York, 1996.
(12) Chesnavich, W. J.; Bowers, M. T. *J. Chem. Phys.* **1977**, *66*, 2306.
(13) Chesnavich, W. J.; Bowers, M. T. *J. Chem. Phys.* **1978**, *68*, 901.
(14) Chesnavich, W. J.; Bowers, M. T. *J. Phys. Chem.* **1979**, *83*, 900.
(15) Chesnavich, W. J.; Bowers, M. T. In *Gas Phase Ion Chemistry*; Bowers, Michael T., Ed.; Academic: New York, 1979; p 119.
(16) Chesnavich, W. J.; Bowers, M. T. *Prog. React. Kinet.* **1982**, *11*, 137.
(17) Grice, M. E.; Song, K.; Chesnavich, W. J. *J. Phys. Chem.* **1986**, *90*, 3503.
(18) Chesnavich, W. J. *J. Chem. Phys.* **1986**, *84*, 2615.
(19) Graul, S. T.; Bowers, M. T. *J. Am. Chem. Soc.* **1994**, *116*, 3875.
(20) Lifshitz, C. *J. Phys. Chem.* **1983**, *87*, 2304.
(21) Teloy, E.; Gerlich, D. *Chem. Phys.* **1974**, *4*, 417.
(22) Gerlich, D. In *State-Selected and State-to-State Ion−Molecule Reaction Dynamics, Part I, Experiment*; Ng, C.-Y., Baer, M., Eds.; Advances in Chemical Physics Series; Wiley: New York, 1992; Vol. 82, p 1.
(23) Ervin, K. M.; Armentrout, P. B. *J. Chem. Phys.* **1985**, *83*, 166.
(24) Truhlar, D. G.; Garrett, B. C.; Klippenstein, S. J. *J. Phys. Chem.* **1996**, *100*, 12771.
(25) Leitner, D. M.; Wolynes, P. G. *Chem. Phys.* **2006**, *329*, 163.
(26) Agbo, J. K.; Leitner, D. M.; Evans, D. A.; Wales, D. J. *J. Chem. Phys.* **2005**, *123*, 124304.
(27) Dunbar, R. C.; McMahon, T. B.; Thoelmann, D.; Tonner, D. S.; Salahub, D. R.; Wei, D. *J. Am. Chem. Soc.* **1995**, *117*, 12819.
(28) Price, W. D.; Williams, E. R. *J. Phys. Chem. A* **1997**, *101*, 8844.
(29) Gioumousis, G.; Stevenson, D. P. *J. Chem. Phys.* **1958**, *29*, 294.
(30) Levine, R. D.; Bernstein, R. B. *J. Chem. Phys.* **1972**, *56*, 2281.
(31) Armentrout, P. B. *Int. J. Mass Spectrom.* **2000**, *200*, 219.
(32) Muntean, F.; Armentrout, P. B. *J. Chem. Phys.* **2001**, *115*, 1213.
(33) Armentrout, P. B. In *Advances in Gas Phase Ion Chemistry*; Adams, N. G.; Babcock, L. M., Eds.; JAI: Greenwich, 1992; Vol. 1, pp 83−119.
(34) Armentrout, P. B. *Int. J. Mass Spectrom.* **2000**, *200*, 219.
(35) Rodgers, M. T.; Armentrout, P. B. In *Comprehensive Coordination Chemistry II: From Biology to Nanotechnology. Volume 2: Fundamentals*; Lever, A. B. P., Ed.; Elsevier: Dordrecht, The Netherlands, 2004; pp 141−158.
(36) Beyer, T. S.; Swinehart, D. F. *Commun. Assoc. Comput. Machinery* **1973**, *16*, 379.
(37) Stein, S. E.; Rabinovitch, B. S. *J. Chem. Phys.* **1973**, *58*, 2438.
(38) Stein, S. E.; Rabinovitch, B. S. *Chem. Phys. Lett.* **1977**, *49*, 183.
(39) Gilbert, R. G.; Smith, S. C. *Theory of Unimolecular and Recombination Reactions*; Blackwell: Oxford, U.K., 1990.
(40) Fernandez-Ramos, A.; Ellingson, B. A.; Meana-Paneda, R.; Marques, J. M. C.; Truhlar, D. G. *Theor. Chem. Acc.* **2007**, *118*, 813.
(41) (a) Light, J. C. *J. Chem. Phys.* **1964**, *40*, 3221. (b) Pechukas, P.; Light, J. C. *J. Chem. Phys.* **1965**, *42*, 3281.
(42) Nikitin, E. E. *Teor. Eksp. Khim.* **1965**, *135*, 144−248; *Theor. Exp. Chem. (Eng. Trans.)* **1975**, *1*, 83, 90, 275.
(43) Chesnavich, W. J.; Bowers, M. T. *J. Phys. Chem.* **1978**, *68*, 901.
(44) Rodgers, M. T.; Ervin, K. M.; Armentrout, P. B. *J. Chem. Phys.* **1997**, *106*, 4499.
(45) Waage, E. V.; Rabinovitch, B. S. *Chem. Rev.* **1970**, *70*, 377.
(46) Loh, S. K.; Lian, L.; Armentrout, P. B. *J. Am. Chem. Soc.* **1989**, *111*, 3167.
(47) Lian, L.; Su, C.-X.; Armentrout, P. B. *J. Chem. Phys.* **1992**, *97*, 4084.
(48) Armentrout, P. B.; Hales, D. A.; Lian, L. In *Advances in Metal and Semiconductor Clusters*; Duncan, M. A., Ed.; JAI: Greenwich, 1994; Vol. 2, pp 1−39.
(49) Lian, L.; Su, C.-X.; Armentrout, P. B. *J. Chem. Phys.* **1992**, *96*, 7542.
(50) Rodgers, M. T.; Armentrout, P. B. *Mass Spectrom. Rev.* **2000**, *19*, 215.
(51) Fraser-Monteiro, M. L.; Fraser-Monteiro, L.; de Wit, J.; Baer, T. *J. Phys. Chem.* **1984**, *88*, 3622.
(52) Muntean, F.; Armentrout, P. B. *J. Phys. Chem. B* **2002**, *106*, 8117.
(53) Lifshitz, C.; Gefen, S. *Org. Mass Spectrom.* **1984**, *19*, 197.
(54) Malinovitch, Y.; Lifshitz, C. *J. Phys. Chem.* **1986**, *90*, 4311.
(55) Le, H. T.; Flammang, R.; Gerbaux, P.; Bouchoux, G.; Nguyen, M. T. *J. Phys. Chem. A* **2001**, *105*, 11582.
(56) More, M. B.; Glendening, E. D.; Ray, D.; Feller, D.; Armentrout, P. B. *J. Phys. Chem.* **1996**, *100*, 1605.
(57) Meyer, F.; Khan, F. A.; Armentrout, P. B. *J. Am. Chem. Soc.* **1995**, *117*, 9740.
(58) Rodgers, M. T.; Armentrout, P. B. *J. Phys. Chem. A* **1997**, *101*, 1238.
(59) Armentrout, P. B.; Rodgers, M. T. *J. Phys. Chem. A* **2000**, *104*, 2238.
(60) Iceman, C.; Armentrout, P. B. *Int. J. Mass Spectrom.* **2003**, *222*, 329.
(61) Angel, L. A.; Ervin, K. M. *J. Phys. Chem. A* **2006**, *110*, 10392.
(62) Muntean, F.; Heumann, L.; Armentrout, P. B. *J. Chem. Phys.* **2002**, *116*, 5593.
(63) Loh, S. K.; Hales, D. A.; Lian, L.; Armentrout, P. B. *J. Chem. Phys.* **1989**, *90*, 5466.
(64) Rodgers, M. T.; Armentrout, P. B. *J. Chem. Phys.* **1998**, *109*, 1787.
(65) Ye, S. J.; Moision, R. M.; Armentrout, P. B. *Int. J. Mass Spectrom.* **2005**, *240*, 233.
(66) Ye, S. J.; Moision, R. M.; Armentrout, P. B. *Int. J. Mass Spectrom.* **2006**, *253*, 288.
(67) Heaton, A. L.; Ye, S. J.; Armentrout, P. B. *J. Phys. Chem. A* **2008**, *112*, 3328.
(68) Amicangelo, J. C.; Armentrout, P. B. *Int. J. Mass Spectrom.* **2001**, *212*, 301.
(69) Cooks, R. G.; Kruger, T. L. *J. Am. Chem. Soc.* **1977**, *99*, 1279.
(70) McLuckey, S. A.; Cameron, D.; Cooks, R. G. *J. Am. Chem. Soc.* **1981**, *103*, 1313.
(71) Armentrout, P. B. *J. Mass Spectrom.* **1999**, *34*, 74.
(72) Muntean, F.; Armentrout, P. B. *J. Phys. Chem. A* **2003**, *107*, 7413.
(73) Muntean, F.; Armentrout, P. B. *Z. Phys. Chem.* **2000**, *214*, 1035.
(74) Orlando, T. M.; Friedmann, A.; Maier, J. P. *J. Chem. Phys.* **1990**, *92*, 7365.
(75) Graul, S. T.; Bowers, M. T. *J. Phys. Chem.* **1991**, *95*, 8328.
(76) Ruan, C.; Yang, Z.; Rodgers, M. T. *Phys. Chem. Chem. Phys.* **2007**, *9*, 5902.
(77) Rannulu, N. S.; Amunugama, R.; Yang, Z.; Rodgers, M. T. J. *Phys. Chem. A* **2004**, *108*, 6385.
(78) Amicangelo, J. C.; Armentrout, P. B. *J. Phys. Chem. A* **2004**, *108*, 10698.
(79) Su, T. *J. Chem. Phys.* **1994**, *100*, 4703.
(80) Hoyau, S.; Norrman, K.; McMahon, T. B.; Ohanessian, G. *J. Am. Chem. Soc.* **1999**, *121*, 8864.
(81) Armentrout, P. B. *J. Chem. Phys.* **2007**, *126*, 234302.
(82) Castleman, A. W., Jr. *Chem. Phys. Lett.* **1978**, *53*, 560.
(83) Koizumi, H.; Armentrout, P. B. *J. Chem. Phys.* **2003**, *119*, 12819.
(84) Ray, D.; Feller, D.; More, M. B.; Glendening, E. D.; Armentrout, P. B. *J. Phys. Chem.* **1996**, *100*, 16117.
(85) More, M. B.; Ray, D.; Armentrout, P. B. *J. Phys. Chem. A* **1997**, *101*, 831.
(86) More, M. B.; Ray, D.; Armentrout, P. B. *J. Phys. Chem. A* **1997**, *101*, 4254.
(87) Koizumi, H.; Muntean, F.; Armentrout, P. B. *J. Chem. Phys.* **2004**, *120*, 756.
(88) Koizumi, H.; Armentrout, P. B. *J. Am. Soc. Mass Spectrom.* **2001**, *12*, 480.
(89) Laskin, J.; Futrell, J. H. *J. Am. Soc. Mass Spectrom.* **2003**, *14*, 1340.
(90) Laskin, J.; Bailey, T. H.; Futrell, J. H. *Int. J. Mass Spectrom.* **2004**, *234*, 89.
(91) Wysocki, V. H.; Joyce, K. E.; Jones, C. M.; Beardsley, R. L. *J. Am. Soc. Mass Spectrom.* **2006**, *19*, 190.
(92) DeTuri, V. F.; Hintz, P. A.; Ervin, K. M. *J. Phys. Chem. A* **1997**, *101*, 5969.
(93) Rodgers, M. T. *J. Phys. Chem. A* **2001**, *105*, 2374.
(94) Graul, S. T.; Squires, R. R. *J. Am. Chem. Soc.* **1990**, *112*, 2517.
(95) Klassen, J. S.; Kebarle, P. *J. Am. Chem. Soc.* **1997**, *119*, 6552.
(96) Wenthold, P. G.; Squires, R. R. *J. Am. Chem. Soc.* **1994**, *116*, 11890.
(97) Hammad, L. A.; Wenthold, P. G. *J. Am. Chem. Soc.* **2000**, *122*, 11203.
(98) Artau, A.; Nizzi, K. E.; Hill, B. T.; Sunderlin, L. S.; Wenthold, P. G. *J. Am. Chem. Soc.* **2000**, *122*, 10667.
(99) Krouse, I. H.; Hao, C.; Check, C. E.; Lobring, K. C.; Sunderlin, L. S.; Wenthold, P. G. *J. Am. Chem. Soc.* **2007**, *129*, 846.
(100) Gerlich, D.; Disch, R.; Scherbarth, S. *J. Chem. Phys.* **1987**, *87*, 350.
(101) Gerlich, D. *J. Chem. Phys.* **1989**, *90*, 3574.

(102) Narancic, S.; Bach, A.; Chen, P. *J. Phys. Chem. A* **2007**, *111*, 7006.
(103) Sowa-Resat, M. B.; Hintz, P. A.; Anderson, S. L. *J. Phys. Chem.* **1995**, *99*, 10736.
(104) Kim, H.-T.; Green, R. J.; Qian, J.; Anderson, S. L. *J. Chem. Phys.* **2000**, *112*, 5717.
(105) Andersen, A.; Muntean, F.; Walter, D.; Rue, C.; Armentrout, P. B. *J. Phys. Chem. A* **2000**, *104*, 692.
(106) Armentrout, P. B.; Kickel, B. L. In *Organometallic Ion Chemistry*, Freiser, B. S., Ed.; Kluwer: Dordrecht, The Netherlands, 1996; pp 1−45.
(107) Shoeib, T.; El Aribi, H.; Siu, K. W. M.; Hopkinson, A. C. *J. Phys. Chem. A* **2001**, *105*, 710.
(108) El Aribi, H.; Shoeib, T.; Ling, Y.; Rodriquez, C. F.; Hopkinson, A. C.; Siu, K. W. M. *J. Phys. Chem. A* **2002**, *106*, 2908.
(109) El Aribi, H.; Rodriquez, C. F.; Shoeib, T.; Ling, Y.; Hopkinson, A. C.; Siu, K. W. M. *J. Phys. Chem. A* **2002**, *106*, 8798.
(110) Sievers, M. R.; Armentrout, P. B. *J. Phys. Chem.* **1995**, *99*, 8135.
(111) Meyer, F.; Armentrout, P. B. *Mol. Phys.* **1996**, *88*, 187.
(112) Yang, Z.; Rannulu, N. S.; Chu, Y.; Rodgers, M. T. *J. Phys. Chem. A* **2008**, *112*, 388.
(113) Rannulu, N. S.; Rodgers, M. T. *J. Phys. Chem. A* **2007**, *111*, 3465.
(114) Carl, D. R.; Moision, R. M.; Armentrout, P. B. *Int. J. Mass Spectrom* **2007**, *265*, 308.
(115) Carl, D. R.; Armentrout, P. B. Work in progress.
(116) Rodgers, M. T.; Armentrout, P. B. *J. Am. Chem. Soc.* **2000**, *122*, 8548.
(117) Rodgers, M. T.; Armentrout, P. B. *J. Am. Chem. Soc.* **2002**, *124*, 2678.
(118) Rodgers, M. T.; Armentrout, P. B. *Acc. Chem. Res.* **2004**, *37*, 989.
(119) Yang, Z.; Rodgers, M. T. *J. Am. Chem. Soc.* **2004**, *126*, 16217.
(120) Yang, Z.; Rodgers, M. T. *Int. J. Mass Spectrom.* **2005**, *241*, 225.
(121) Yang, Z.; Rodgers, M. T. *J. Phys. Chem. A* **2006**, *110*, 1455.
(122) Heaton, A. L.; Moision, R. M.; Armentrout, P. B. *J. Phys. Chem. A* **2008**, *112*, 3319.
(123) Ye, S. J.; Clark, A. A.; Armentrout, P. B. *J. Phys. Chem. B* **2008**, *112*, 10291.
(124) Heaton, A. L.; Armentrout, P. B. *J. Am. Chem. Soc.* **2008**, *130*, 10227.
(125) Heaton, A. L.; Armentrout, P. B. *J. Phys. Chem. A*, in press.
(126) Ruan, C.; Huang, H.; Rodgers, M. T. *J. Am. Soc. Mass Spectrom.* **2008**, *19*, 305.
(127) Ruan, C.; Huang, H.; Rodgers, M. T. *J. Phys. Chem. A* **2007**, *111*, 13521.
(128) Ye, S. J.; Armentrout, P. B. *J. Phys. Chem. A* **2008**, *112*, 3587.
(129) More, M. B.; Ray, D.; Armentrout, P. B. *J. Am. Chem. Soc.* **1999**, *121*, 417.
(130) Ye, S. J.; Moision, R. M.; Armentrout, P. B. *Int. J. Mass Spectrom.* **2005**, *240*, 233.
(131) Ye, S. J.; Moision, R. M.; Armentrout, P. B. *Int. J. Mass Spectrom.* **2006**, *253*, 288.
(132) Hinderling, C.; Feichtinger, D.; Plattner, D. A.; Chen, P. *J. Am. Chem. Soc.* **1997**, *119*, 10793.
(133) Arndtsen, B. A.; Bergman, R. G. *Science* **1995**, *270*, 1970.
(134) Burger, P.; Bergman, R. G. *J. Am. Chem. Soc.* **1993**, *115*, 10462.
(135) Hammad, L. A.; Gerdes, G.; Chen, P. *Organometallics* **2005**, *24*, 1907.
(136) Moret, M.-E.; Chen, P. *Organometallics* **2007**, *26*, 1523.
(137) Zhang, X.; Narancic, S.; Chen, P. *Organometallics* **2005**, *24*, 3040.
(138) Zocher, E.; Dietiker, R.; Chen, P. *J. Am. Chem. Soc.* **2007**, *129*, 2476.
(139) Zocher, E.; Sigrist, R.; Chen, P. *Inorg. Chem.* **2007**, *46*, 11366.
(140) Ochterski, J. W.; Petersson, G. A.; Montgomery, J. A. *J. Chem. Phys.* **1996**, *104*, 2598.
(141) Rodgers, M. T.; Armentrout, P. B. *Int. J. Mass Spectrom.* **2007**, *267*, 167.
(142) Armentrout, P. B.; Griffin, J. B.; Conceição, J. In *Progress in Physics of Clusters*; Chuev, G. N., Lakhno, V. D., Nefedov, A. P., Eds.; World Scientific: Singapore, 1999; pp 198−225
(143) Armentrout, P. B. *Annu. Rev. Phys. Chem.* **2001**, *52*, 423.
(144) Armentrout, P. B. *Eur. J. Mass Spectrom.* **2003**, *9*, 531.
(145) Bell, R. C.; Zemski, K. A.; Justes, D. R.; Castleman, A. W., Jr. *J. Chem. Phys.* **2001**, *114*, 798.
(146) Liu, F.; Armentrout, P. B. *J. Chem. Phys.* **2005**, *122*, 194320.
(147) Conceição, J.; Loh, S. K.; Lian, L.; Armentrout, P. B. *J. Chem. Phys.* **1996**, *104*, 3976.
(148) Conceição, J.; Liyanage, R.; Armentrout, P. B. *Chem. Phys.* **2000**, *262*, 115.
(149) Liyanage, R.; Conceição, J.; Armentrout, P. B. *J. Chem. Phys.* **2002**, *116*, 936.
(150) Liu, F.; Liyanage, R.; Armentrout, P. B. *J. Chem. Phys.* **2002**, *117*, 132.
(151) Ervin, K. M. *Int. Rev. Phys. Chem.* **2001**, *20*, 127.
(152) Grushow, A.; Ervin, K. M. *J. Chem. Phys.* **1997**, *106*, 9580.
(153) Spasov, V. A.; Ervin, K. M. *J. Chem. Phys.* **1998**, *109*, 5344.
(154) Grushow, A.; Ervin, K. M. *J. Am. Chem. Soc.* **1995**, *117*, 11612.
(155) Shi, Y.; Spasov, V. A.; Ervin, K. M. *Int. J. Mass Spectrom.* **2001**, *204*, 197.
(156) Spasov, V. A.; Shi, Y.; Ervin, K. M. *Chem. Phys.* **2000**, *262*, 75.
(157) Santa-Nokki, T.; Häkkinen, H. *Chem. Phys. Lett.* **2005**, *406*, 44.
(158) Shi, Y.; Spasov, V. A.; Ervin, K. M. *J. Chem. Phys.* **1999**, *111*, 938.
(159) Spasov, V. A.; Lee, T.-H.; Ervin, K. M. *J. Chem. Phys.* **2000**, *112*, 1173.
(160) Shvartsburg, A. A.; Ervin, K. M.; Frederick, J. H. *J. Chem. Phys.* **1996**, *104*, 8458.
(161) Shvartsburg, A. A.; Frederick, J. H.; Ervin, K. M. *J. Chem. Phys.* **1996**, *104*, 8470.
(162) Dalleska, N. F.; Honma, K.; Armentrout, P. B. *J. Am. Chem. Soc.* **1993**, *115*, 12125.
(163) Cunningham, A. J.; Payzant, A. D.; Kebarle, P. *J. Am. Chem. Soc.* **1972**, *94*, 7627.
(164) Lau, Y. K.; Ikuta, S.; Kebarle, P. *J. Am. Chem. Soc.* **1982**, *104*, 1462.
(165) Meot-Ner, M.; Speller, C. V. *J. Phys. Chem.* **1986**, *90*, 6616.
(166) Hiraoka, K.; Takimoto, H.; Yamabe, S. *J. Phys. Chem.* **1986**, *90*, 5910.
(167) Honma, K.; Armentrout, P. B. *J. Chem. Phys.* **2004**, *121*, 8307.
(168) Aribi, H. E.; Rodriquez, C. F.; Almeida, D. R. P.; Ling, Y.; Mak, W. W.-N.; Hopkinson, A. C.; Siu, K. W. M. *J. Am. Chem. Soc.* **2003**, *125*, 9229.
(169) El Aribi, H.; Orlova, G.; Rodriquez, C. F.; Almeida, D. R. P.; Hopkinson, A. C.; Siu, K. W. M. *J. Phys. Chem. B* **2004**, *108*, 18743.
(170) Yang, Z.; Ruan, C.; Ahmed, H. H.; Rodgers, M. T. *Int. J. Mass Spectrom.* **2007**, *265*, 388.
(171) Heaton, A. L.; Ye, S. J.; Armentrout, P. B. Work in progress.
(172) DeTuri, V. F.; Ervin, K. M. *J. Phys. Chem. A.* **1999**, *103*, 6911.
(173) Angel, L. A.; Ervin, K. M. *J. Phys. Chem. A* **2006**, *110*, 10392.
(174) Nix, M. G. D.; Devine, A. L.; Cronin, B.; Dixon, R. N.; Ashfold, M. N. R. *J. Chem. Phys.* **2006**, *125*, 133318.
(175) Angel, L. A.; Ervin, K. M. *J. Phys. Chem. A.* **2004**, *108*, 8345.
(176) Akin, F. A.; Ervin, K. M. *J. Phys. Chem. A* **2006**, *110*, 1342.
(177) Wenthold, P. G. *J. Phys. Chem. A* **2000**, *104*, 5612.
(178) Poutsma, J. C.; Upshaw, S. D.; Squires, R. R.; Wenthold, P. G. *J. Phys. Chem. A* **2002**, *106*, 1067.
(179) Liu, X.; Gross, M. L.; Wenthold, P. G. *J. Phys. Chem. A* **2005**, *109*, 2183.
(180) Lardin, H. A.; Nash, J. J.; Wenthold, P. G. *J. Am. Chem. Soc.* **2002**, *124*, 12612.
(181) Hammad, L. A.; Wenthold, P. G. *J. Am. Chem. Soc.* **2001**, *123*, 12311.
(182) Nizzi, K. E.; Pommerening, C. A.; Sunderlin, L. S. *J. Phys. Chem. A* **1998**, *102*, 7674.
(183) Heil, T. E.; Check, C. E.; Lobring, K. C.; Sunderlin, L. S. *J. Phys. Chem. A* **2002**, *106*, 10043.
(184) Check, C. E.; Lobring, K. C.; Keating, P. R.; Gilbert, T. M.; Sunderlin, L. S. *J. Phys. Chem. A* **2003**, *107*, 8961.
(185) Gailbreath, B. D.; Pommerening, C. A.; Bachrach, S. M.; Sunderlin, L. S. *J. Phys. Chem. A* **2000**, *104*, 2958.
(186) Bachrach, S. M.; Hayes, J. M.; Check, C. E.; Lee, S.; Sunderlin, L. S. *J. Phys. Chem. A* **2001**, *105*, 9595.
(187) Lobring, K. C.; Hao, C.; Forbes, J. K.; Ivanov, M. R. J.; Bachrach, S. M.; Sunderlin, L. S. *J. Phys. Chem. A* **2003**, *107*, 11153.
(188) Hao, C.; Kaspar, J. D.; Check, C. E.; Lobring, K. C.; Gilbert, T. M.; Sunderlin, L. S. *J. Phys. Chem. A* **2005**, *109*, 2026.
(189) Goebbert, D. J.; Hernandez, H.; Francisco, J. S.; Wenthold, P. G. *J. Am. Chem. Soc.* **2005**, *127*, 11684.
(190) Aristov, N.; Armentrout, P. B. *J. Phys. Chem.* **1986**, *90*, 5135.
(191) Sievers, M. R.; Chen, Y.-M.; Armentrout, P. B. *J. Chem. Phys.* **1996**, *105*, 6322.
(192) Zhang, X.-G.; Armentrout, P. B. *J. Phys. Chem. A* **2003**, *107*, 8904–8915.
(193) Akin, F. A.; Ree, J.; Ervin, K. M.; Shin, H. K. *J. Chem. Phys.* **2005**, *123*, 064308.
(194) Fisher, E. R.; Kickel, B. L.; Armentrout, P. B. *J. Phys. Chem.* **1993**, *97*, 10204.
(195) Ricca, A.; Bauschlicher, C. W. *J. Phys. Chem. A* **1998**, *102*, 876.

(196) Sawilosky, E. F.; Klippenstein, S. J. *J. Phys. Chem. A* **1998**, *102*, 9811.

(197) Chesnavich, W. J.; Bass, L.; Su, T.; Bowers, M. T. *J. Chem. Phys.* **1981**, *74*, 2228.

(198) Jia, B.; Angel, L. A.; Ervin, K. M. *J. Phys. Chem. A.* **2008**, *112*, 1773.

(199) Ryzhov, V.; Yang, Y.-C.; Klippenstein, S. J.; Dunbar, R. C. *J. Phys. Chem. A* **1998**, *102*, 8865.

(200) Rodgers, M. T.; Armentrout, P. B. *Int. J. Mass Spectrom.* **1999**, *185*−*187*, 359.

(201) Ervin, K. M.; DeTuri, V. F. *J. Phys. Chem. A* **2002**, *106*, 9947.

JP805343H